Some biochemcial studies on the human lens nucleus

Xiaojia Wei
University of Wollongong

SOME BIOCHEMCIAL STUDIES ON THE HUMAN LENS NUCLEUS

Wei Xiaojia (Eric), B.Sc., M.Sc.

This thesis is presented as full requirements for the award of a

Master of Science by Research (Medicinal Chemistry)

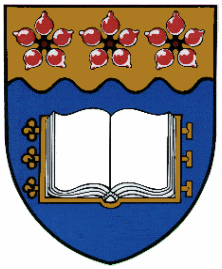

Supervisor: Professor Roger Truscott

Department of Chemistry

University of Wollongong

Wollongong, Australia

March, 2006

CERTIFICATION

I, Xiaojia Wei, declare that this thesis, submitted in full fulfillment of the requirements for the award of Master of Science by Research, in the Department of Chemistry, University of Wollongong, is wholly my own work unless otherwise referenced or acknowledged. The document has not been submitted for qualifications at any other academic institution.

Xiaojia Wei

29/03/2006

ACKNOWLEDGEMENTS

I would like to thank everyone who helped me throughout the duration of this research project.

To my supervisor, Professor Roger Truscott, for his advice, support and guidance, and the valuable time spent helping me.

To Dr John Korth, Dr Todd Mitchell, Assoc. Prof. Will Price and Prof. Tony Hulbert, for their patience, support and help.

To Anastasia, Ines, Jane, Karl, Madge, Michael, Nicole, Peter, Yoke and all past and present members of the Truscott research group, their support and assistance was much appreciated, and also their friendship.

To the Chemistry Department, the social nature of the department provides a very comfortable surrounding to work in.

To my friends Gareth and Carolyn for proof reading.

To my family, for their support, encouragement and endless love.

TABLE OF CONTENTS

LIST OF ABBREVIATIONS

The following abbreviations were used in this thesis

ACRF	Australian Cataract Research Foundation
ADP	Adenosine Diphosphate
Ag/AgCl	Silver/Silver Chloride
AHBG	4-(2-amino-3-hydroxyphenyl-4-oxobutanoic acid glucoside
AQP0	Aquaporin0
ARNC	Age-related Nuclear cataract
ATP	Adenosine Triphosphate
BCA	Bicinchoninic Acid
BSA	Bovine Serum Albumin
$CHCl_3$	Chloroform
CoQ	CoenzymeQ
CytC	CytochromeC
DC Voltage	Direct Current Voltage
DI	Direct insertion
DNP	2,4-dinitrophenol
DTNB	5,5'-dithiobis-(nitrobenzoic acid)
EDTA	Ethylenediaminetetraacetic Acid
EI Ionization	Electron Impact Ionization
ESI	Electrospray Ionization
ETC	Electron Transport Chain
FCCP	Carbonylcyanide-p-trifluoromethoxyphenyl hydrozone
GSH	Glutathione (reduced form)
GSSG	Glutathione (oxidized form)
HEPES	4-(2-hydroxyethyl)-1-piperazineethanesulfonic acid
HMM	High Molecular Mass
HPLC	High Performance Liquid Chromatography
IAA	Iodoacetic Acid
IOL	Intraocular Lens
KCl	Potassium Chloride
Kyn	Kynurenine
MALDI	Matrix Assisted Laser Desorption Ionization
MeOH	Methanol
m/z	Mass to Charge
NADH	Nicotinamide Adenine Dinucleotide (reduce form)

NMR	Nuclear Magnetic Resonance
O_2	Molecular Oxygen/Oxygen
PBS	Phosphate-buffered Saline
pO_2	Partial Pressure of Oxygen
PSH	Peotein Sulphydryl
R^2	Regression
Rf Voltage	Radio Frequency Oscillation Voltage
ROS	Reactive Oxygen Species
SDS	Sodium Dodecyl Sulphate
SIM	Selected Ion Monitoring
TCA	Trichloracetic Acid
Tris-HCl	Tris(hydroxymethyl)aminomethane
UV	Ultra Violet
WR	Working Reagent
WS	Water Soluble
y.o.	Years Old

ABSTRACT

Barrier[16] formation has been shown to occur in the lens with age. It is important to understand the physiological changes in the lens that occur upon the formation of the barrier and their implication on the onset of cataract and presbyopia (old man's eyes). In this study, three factors related to the formation of the barrier were investigated: diffusion rate changes in the lens nucleus, oxygen consumption and cholesterol compositional changes in the lens with age.

A Franz Cell was used to measure the diffusion rate changes in the nucleus of the human lens. No significant differences in the rate of diffusion between young and old lenses could be detected with this technique.

The role of protein sulphydryls as secondary oxygen consumers was also studied. It was shown that protein sulphydryls reacted readily with oxygen, suggesting that protein sulphydryls are a secondary O_2-consumption system in the center of the lens. Mitochondria are the primary oxygen consumers in the lens.

A technique for the quantification of cholesterol in lipid extracts was developed. Results obtained were comparable to published results using traditional methods. The concentration of cholesterol in the young human lens was found to be approximately 3-fold greater than that of the bovine, ovine and porcine lenses, and ~5 times greater

than in the gallinaceous lens. These differences were even more pronounced when an elderly human lens was examined. The nucleus of the human lens was found to have a higher level of cholesterol content than that in the cortex and the concentration of cholesterol also exhibited a significant increase with age in both nuclear and barrier regions.

Chapter 1: General Introduction

1.1. The Human Lens

The human lens is a transparent and highly refractive structure located at the anterior portion of the eye, between the iris and the vitreous body (**Figure 1-1**). The lens focuses light onto the retina at the back of the eye and adjusts the eye's focus so vision can be clear.[1] A secondary function of the lens is to protect the sensory section of the eye, the retina, from UV radiation.[2]

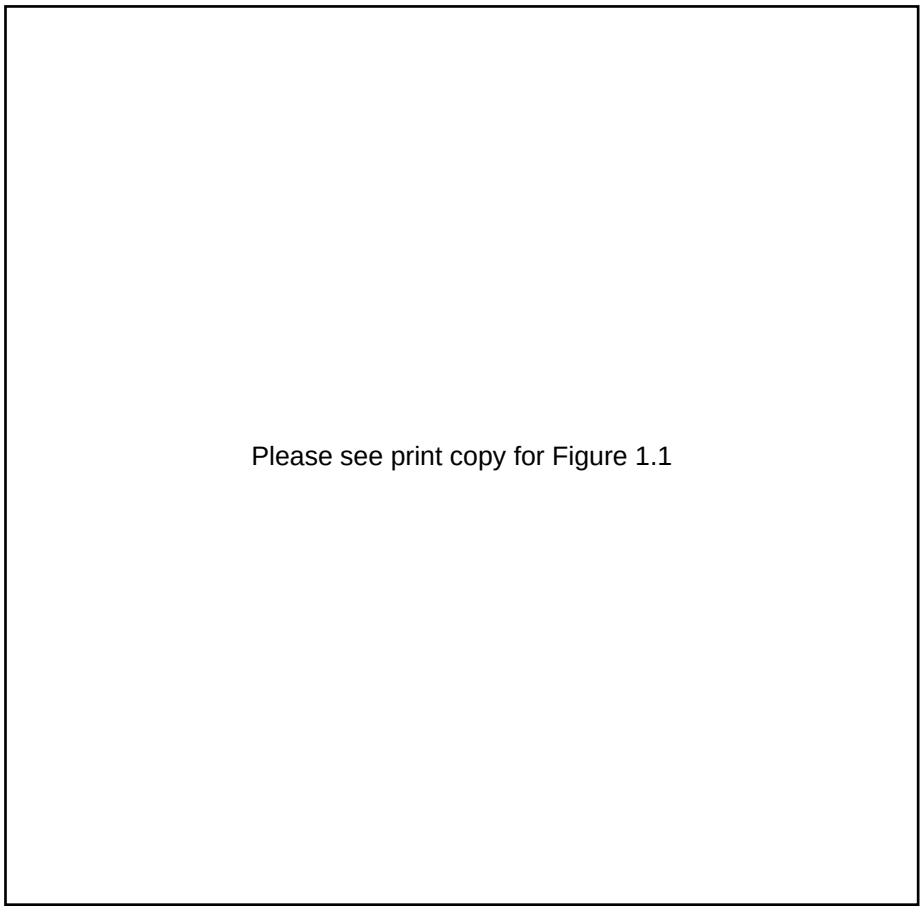

***Figure 1-1*: The anatomy of the human eye, the lens centrally located at the anterior portion of the eye between the iris and the vitreous body.**[73]

The human lens is comprised of approximately 65% water and 35% protein by weight, thus having the highest protein concentration of any tissue. The high protein concentration is necessary to obtain the refractive index needed for focusing light and maintenance of the lens transparency.[3]

1.1.1. Development of the Human Lens

The human lens is comprised of two kinds of cells: epithelial and fibre cells (**Figure 1-2**).[4] Throughout the life of an individual, the lens grows by building up layers of fibre cells around the original nucleus, which is present at birth. In the center of the lens, there is no protein turnover during an individual's lifetime, resulting in the lens steadily increasing in weight and thickness with age.[5] Thus, the nuclear region of the lens is increasingly isolated from the diffusion of nutrients and antioxidants from the epithelium, leading to the accumulation of a variety of post-translational modifications.[6]

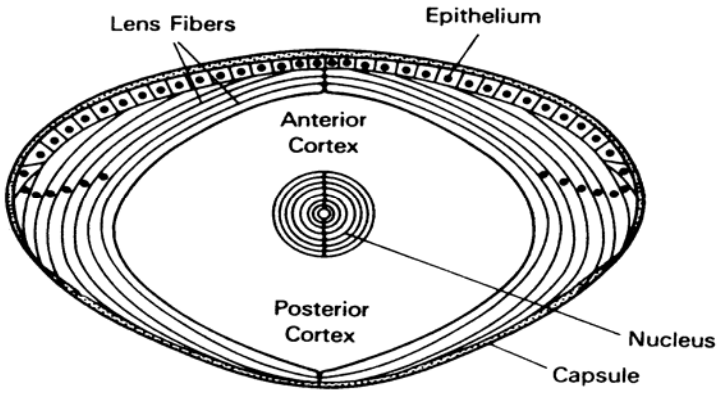

***Figure 1-2*: Cross section of the human lens showing the concentric layers of fiber cells.**

1.1.2. Composition of the Human Lens

1.1.2.1. Proteins in the Lens

The lens consists of structural proteins, called crystallins, which make up over 90% of the lens protein. Crystallins are water-soluble and essential for facilitating the proper transmission of light. In the human lens, the crystallins are divided into three major families, the α-, β- and γ-crystallins, which exist in approximately equal proportions. Each major crystallin group is then divided further into subunits. For example, α-crystallin is comprised of αA- and αB-crystallin subunits. The β- and γ-crystallins are homologous to each other, and are grouped together as a superfamily of β–γ crystallins.[7, 8] α-Crystallin is a small heat shock protein and acts as a molecular chaperone in the lens.

Chaperone proteins are a specialized group of proteins that promote correct folding, by binding to exposed hydrophobic sites on a polypeptide. This limits possible harmful interactions that may lead to aggregation and precipitation. In the human lens, α-crystallin plays a significant role, regulating harmful aggregates that may lead to opacification, by binding unfolding proteins.[9, 10] α-Crystallin forms oligomers, consisting of a range of polypeptide subunits, with molecular weights over 500 kDa. The β-crystallins form oligomers with molecular weights 40 kDa-200 kDa, while the γ-crystallins are monomeric, having a molecular weight of ~20 kDa.[11, 12]

The extremely long lifetime of crystallins makes them susceptible to a wide variety of covalent modifications. These modifications include phosphorylation, aggregation, deamidation, chain cleavages, racemization, pigmentation and glycation.[13] It is recognized that these age-related changes in the human lens are probable factors in the development of lens opacification, i.e. cataract.

1.1.2.2. UV-Filters

The human lens also contains a number of low molecular weight UV-filters. The function of the UV-filters is to act as intraocular filters against UV-photo-damage to the lens and the retina. The UV-filters absorb most of the UV light transmitted by the cornea between 295 and 400 nm with a maximum absorption between 360 and 370 nm.[14] The UV-filters found in the lens, occur in different concentrations. L-3-hydroxykynurenine *O*-B-D-glucoside (3OHKG) **[1]** being the most prevalent, present in the mM range. 4-(2-Amino-3-hydroxyphenyl -4-oxobutanoic acid glucoside (AHBG) **[2]** is the second most abundant, found at 0.2 to 1.3 mM, followed by L-kynurenine (Kyn) **[3]** and L-3-hydroxykynurenine (3OHKyn) **[4]** (**Figure 1-3**). Recent studies have revealed that UV-filters are involved in the modification of older human lens crystallins and also covalently interact with glutathione (GSH) to give GSH-3OHKG after middle age.[15]

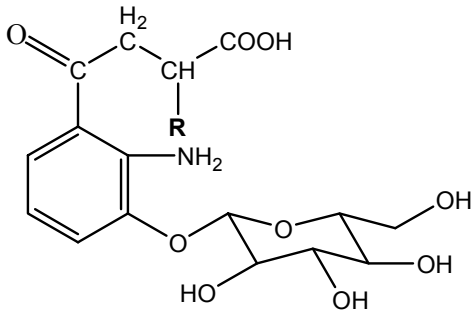

[**1**] **R** = NH_2

[**2**] **R** = H

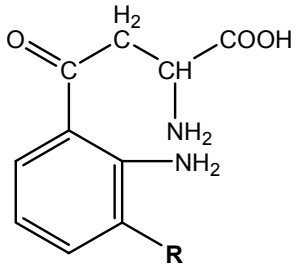

[**3**] **R** = H

[**4**] **R** = OH

***Figure 1-3*: The structure of UV-filters in the human lens.**

1.1.2.3. Antioxidants

Antioxidants are another group of important small molecular weight compounds found in the mammalian lens. The major antioxidants in the lens are glutathione (GSH) and ascorbic acid. GSH is synthesized in the outer cortical region. The glutathione cycles between nuclear and outer cortical regions (**Figure 1-4**) and is thought to be the most important antioxidant system in the lens. The cycle between GSH, which is the reduced form of glutathione, and GSSG, an oxidized form (**Figure 1-5**), is essential to maintaining protein thiols in the reduced state, which in turn prevents the formation of protein aggregates. Ascorbic acid is important for prevention of lipid peroxidation in the lens, due to its ability to scavenge reactive oxygen species (ROS).[16]

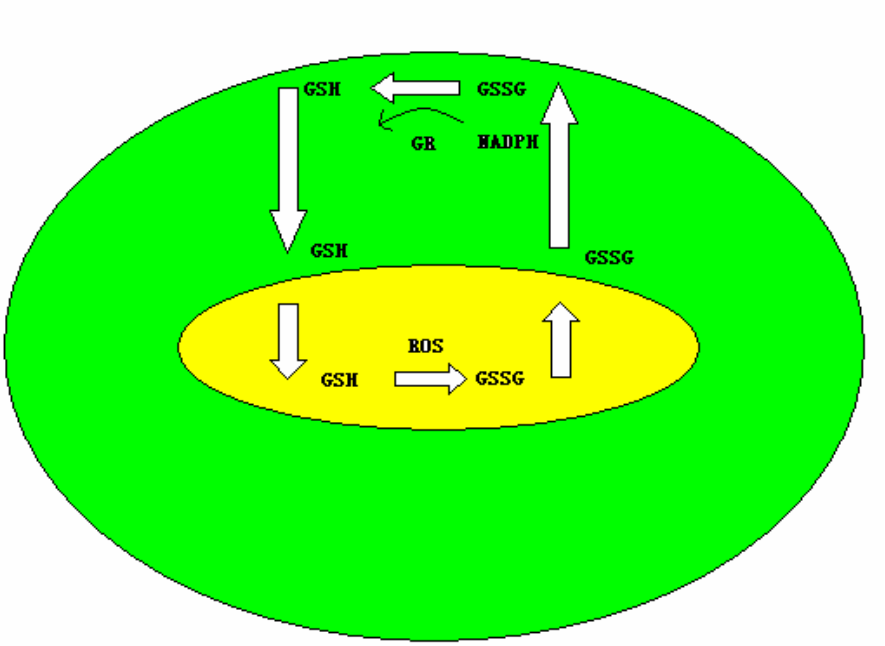

***Figure 1-4*: The diagram shows the GSH/GSSG cycle between nuclear and outer cortical region in the human lens. GR = Glutathione reductase.**

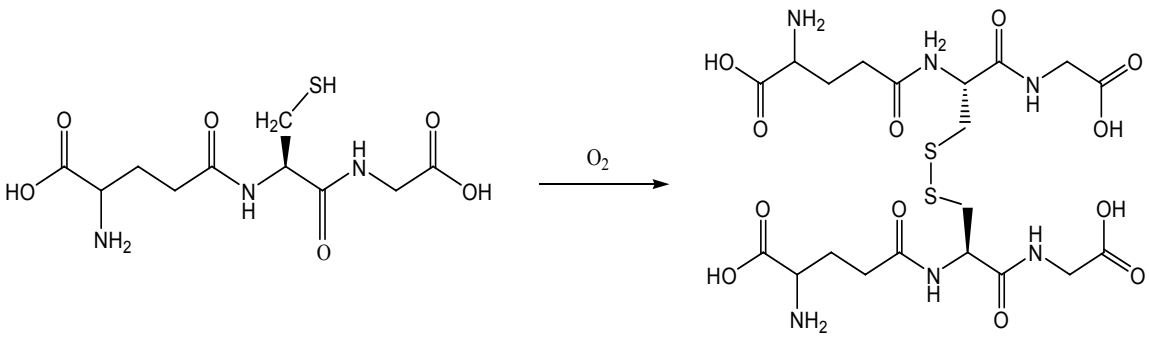

***Figure 1-5*: The reduced form of glutathione (GSH) oxidized to GSSG.**

1.2. Human Cataract

Cataract is the major cause of blindness worldwide. Cataract is the clouding of the normally transparent lens leading to impairment or loss of vision (**Figure 1-6**). The

lens normally becomes yellow with age but remains transparent.

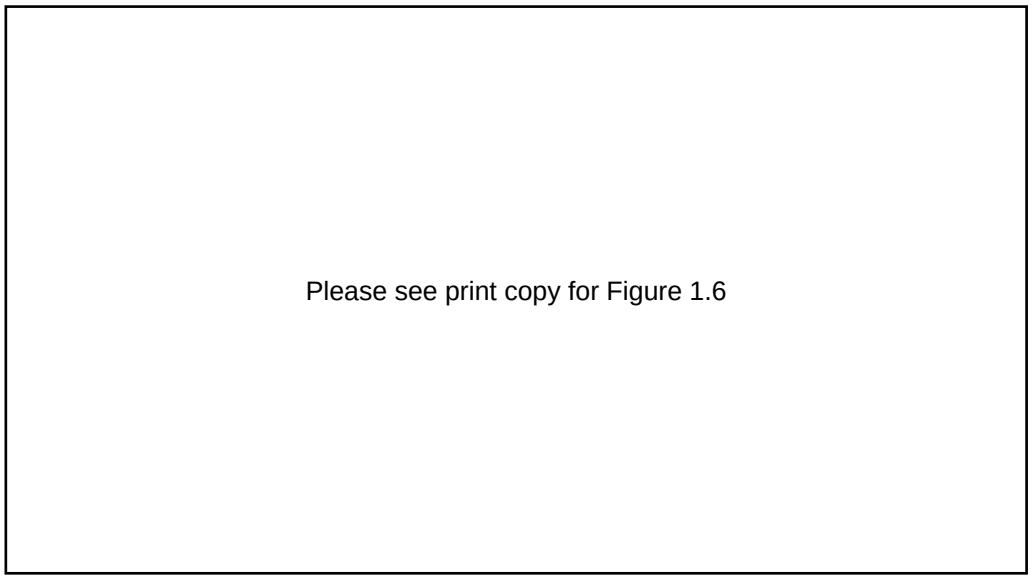

***Figure 1-6*: Comparison of normal vision (*A*) and vision with cataract (*B*).**[74]

1.2.1. Categorising Cataract Type

Cataract can be classified by the location of the opacity within the lens (e.g. cortical or nuclear), or by the age of onset (e.g. juvenile, senile or congenital).[19] There are various factors associated with the formation of cataract, including family history, medical problems, diabetes, injury to the eye, medications, steroids, possibly long-term exposure to sunlight, lack of vitamins in the diet and various eye surgeries.

At the onset of nuclear cataract, the colour of the lens gradually darkens, turning a variety of shades of brown (**Figure 1-7**). A type I cataract is a cortical cataract, which is located in the outer portion of the lens. Type II to type V cataracts are different severities of nuclear cataracts, with type V being the most severe.[17, 18]

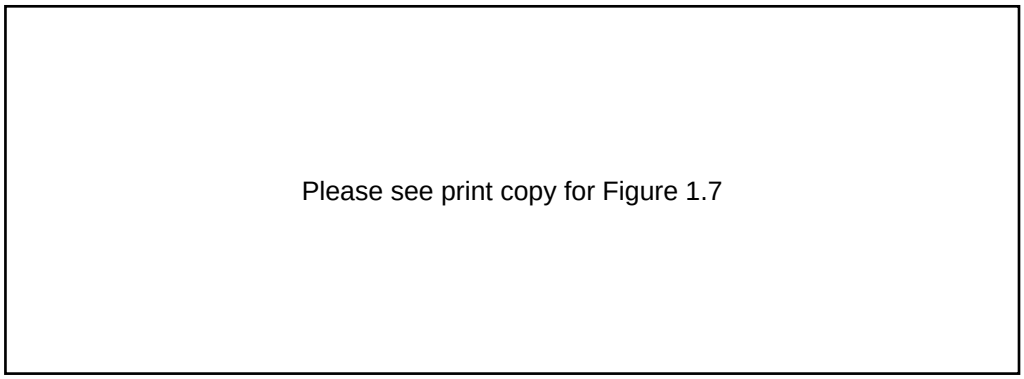

***Figure 1-7*: Classification system of the different types of nuclear cataract. A normal lens is shown for comparison. Photo courtesy of Prof. George Duncan.**

1.2.2. Age-Related Nuclear Cataract (ARNC)

This study focuses on age-related nuclear cataract (ARNC), the major type of cataract causing blindness in the elderly throughout the world. ANRC is a nuclear cataract and is characterised by colouration in the center of the lens. At present, there are no medical treatments, dietary supplements or exercises that have been shown to be effective in the prevention of ARNC. Surgery at present is the only method to cure cataract. Cataract surgery involves the removal of the opaque lens and subsequent replacement with an artificial intraocular lens (IOL).[20] This is very costly and due to the increasing aging population, it is important to develop effective drugs to combat this disease. The major barrier in developing an efficacious drug treatment to prevent or cure cataract is the current lack of knowledge regarding cataract formation.

1.2.3. The Lens Barrier

Numerous factors are associated with the formation of nuclear cataract (**1.2.1.**), however, age remains the major risk factor. As previously mentioned, the nuclear region of the lens depends crucially upon the outer cortical region and epithelial cells for nutrients and antioxidants, but, with age, due to the formation of a proposed lens barrier, it becomes increasingly isolated from these important supplies. Therefore, understanding how transport in the lens changes with age becomes a crucial issue to reveal the onset of ARNC. The barrier theory was introduced by the Australian Cataract Research Foundation (ACRF) several years ago. It hypothesises that at middle age, a barrier forms at the cortical-nuclear interface which impedes the movement of small molecules (e.g. water, antioxidants and nutrients) in the lens, consequently leading to a decrease in the level of crucial small molecules in the nucleus (**Figure 1-8**).[16, 21] The implication of such a process may provide answers as to why the onset of cataract becomes more likely with age.

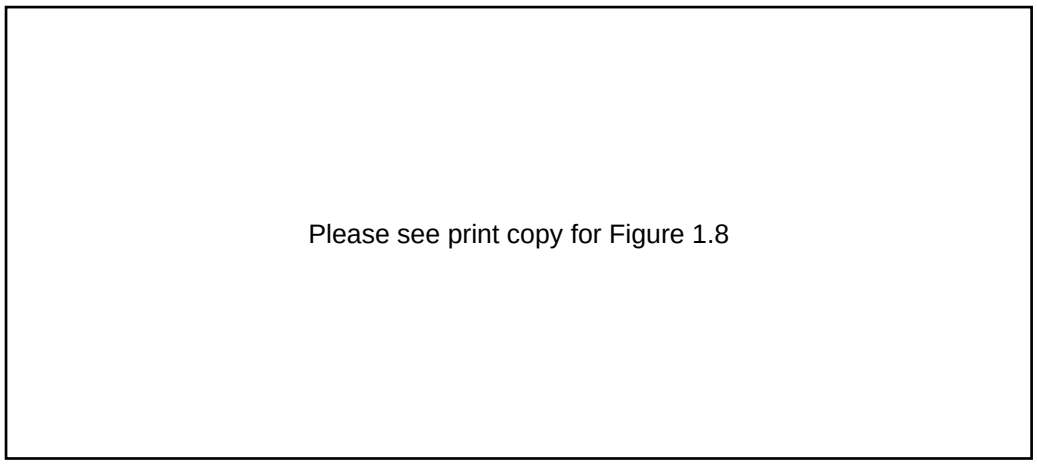

***Figure 1-8*: Autoradiographs of axial sections of a young (*A*) and an old (*B*) human lens following incubation for 48 hours with [^{35}S] cysteine, which shows a barrier impedes cysteine transport between the nuclear and cortical region. Red is equivalent to back ground and blue approximately a thousand disintegrations per 50 µm (10× background).**[16]

Experimental evidence of this barrier has been observed, however, the reason for its formation is still unknown. Two hypotheses for the formation of the barrier have been suggested, the membrane channels become blocked in the region between cortex and nucleus and/or the nucleus changes in physical nature with age. Some studies have shown that marked changes take place in the physical/chemical properties of the human lens with age. These include increases in stiffness,[5] fluorescence and light scatter of the lens and a possible decrease in the refractive index of the nucleus.[22]

In order to understand the mechanism of barrier formation and its role on the onset of nuclear cataract, it is necessary to investigate aging of the lens. Diffusion rate in the nuclear region, oxygen consumption and cholesterol content in the lens were analysed in this study as three indicators of the aging process.

Chapter 2: Diffusion in the Lens

2.1. Introduction

2.1.1. Physical Properties Change with Age

A number of studies have shown that some changes take place in the properties of the human lens with age. These include an increase in fluorescence and light scatter, a decrease in elasticity of lens and a possible decrease in the refractive index of the nucleus.[22] Recent research by the ACRF found an enormous increase in stiffness in the lens nucleus, which is possibly linked to barrier formation. This hardening of the lens is the primary cause of presbyopia (the inability to focus on nearby objects with age).[5] Diffusion changes in the nuclear region of the lens with age were investigated as another possible link to barrier formation.

2.1.2. Diffusion

Diffusion is an important process that underlies the passive movement of materials into and out of cells as well as the traffic of certain molecules within the cell. Diffusion is also the most important mechanism that supplies the organism with oxygen, water, nutrients and other requirements.[23] In the lens, these requirements include antioxidants, UV-filters, nutrients as previously mentioned, which are generated in the anterior of

the lens, and transferred into the nuclear region.[24] In scientific research, diffusion measurements has been used to characterise normal and pathological tissues as well as the penetrability of medicines and cosmetics. The force driving diffusion is generated by the presence of a concentration difference between two regions and operates in the following manner: molecules always move (unless there is an obstruction) from regions of higher concentration to regions of lower concentration. The diffusion rate is the index used to measure diffusion. A rate is a quantity expressed per unit of time, and diffusion rate is expressed as the movement of a certain number of molecules per time. Generally, the diffusion rate (D, mole/min) depends primarily on three factors: the surface area (S) across which the exchange occurs; the permeability of the membrane or tissue through with diffusion will occur (proportional to its thickness, L) and the difference in the concentration (ΔC) between the two sides of the membrane or tissue (**Equation 2-1**).[23]

$$D = S \bullet \Delta C / L$$

***Equation 2-1*: The equation illustrates the relationship of diffusion rate (D) and surface area (S), concentration (ΔC) and thickness (L).**

In order to investigate the diffusion of small molecules in the human lens with age, a small molecule tracer needs to be used, which does not interact with proteins. Tritiated water was used due to its sensitivity of detection. In the lens, water moves through aquaporin0 (AQP0) channels.[25] In addition, NMR imaging has shown that the

diffusion of water is reduced in older human lens nuclei.[21] Radioactive amino acids can be used to detect whether other channels, such as, connexons function less in older lenses.[25, 26] Diffusion rates were determined with tritiated water by measuring the increase of the scintillation counts in the receptor chamber of a modified Franz Cell (**Figure 2-1**) over a fixed time period. If the counts (dpm) are plotted against time, the slope of the resulting line represents the diffusion rate, which is a measure of the quantity of substance crossing membranes per unit time.

2.1.3. Purpose and Aims

The purpose of this part of the study was to investigate changes in diffusion in the nuclear regions of the human lens with age. This research project involves a novel approach to investigate the movement of small molecules in the human lens. The results may lead to a greater understanding of the physical changes occurring in the human lens with age, especially in the nuclear region, and may add to our understanding of barrier formation. The results may also have important consequences in understanding the formation of ARNC, and its prevention.

This project aims to examine and compare changes in diffusion in the nuclear regions of the human lens with age.

2.2. Experimental

2.2.1. Materials

2.2.1.1. Biological Samples

Porcine eyes were obtained from CrownPork, Strathfield, NSW, Australia. Bovine and ovine eyes were obtained from Wollondilly Abattoirs Pty. Ltd., Picton, NSW. Human lenses were obtained from the Sydney Eye Bank, Sydney, NSW. Whole eyes and lenses were transported to the laboratory on ice, and lenses were immediately extracted from the eyes by micro dissection. All preparations were conducted on ice. The lenses were stored at –80^{o}C until used. The work was approved by the human research ethics committee at the University of Wollongong.

2.2.1.2. Chemicals and Solutions

The Radioactive Isotope

Tritiated water (5.0 mCi/mL) was supplied from Amersham Biosciences, UK. 5 μL of tritiated water was diluted in 10 mL PBS (protocol see below) and used as the diffusion solution (2.5 μCi/mL/expt.). The diluted tritiated water/PBS mixture was stored at 4^{o}C until used.

Phosphate-buffered Saline (PBS)

Sodium chloride (NaCl) (0.81 g) and potassium chloride (KCl) (0.015 g) were dissolved in 10 mM phosphate buffer (100 mL). The final concentration of NaCl and KCl in solution was 137 mM and 2 mM respectively. The pH value of PBS is 7.4 +/- 0.1. PBS was stored at 4^{o}C until used.

2.2.2. Apparatus

2.2.2.1. Modified Franz Cell

The Franz Cell investigates permeation through membranes.[27] The Franz Cell is a vertical glass diffusion cell, and has two glass compartments, the donor and receptor compartments. The membrane specimen is placed between the two compartments.[28] Modifications were made to the Franz Cell in order to investigate the column shape lens tissue specimen (**Figure 2-1**). The donor compartment was used for a "plug" of lens tissue. The diffusion solution containing tritiated water was added to the Eppendorff tip (**Figure 2-1**). A spacer was designed to adjust the height of Eppendorff tip, and to keep the end of the tip at the same distance (2 mm) from the membrane in each experiment.

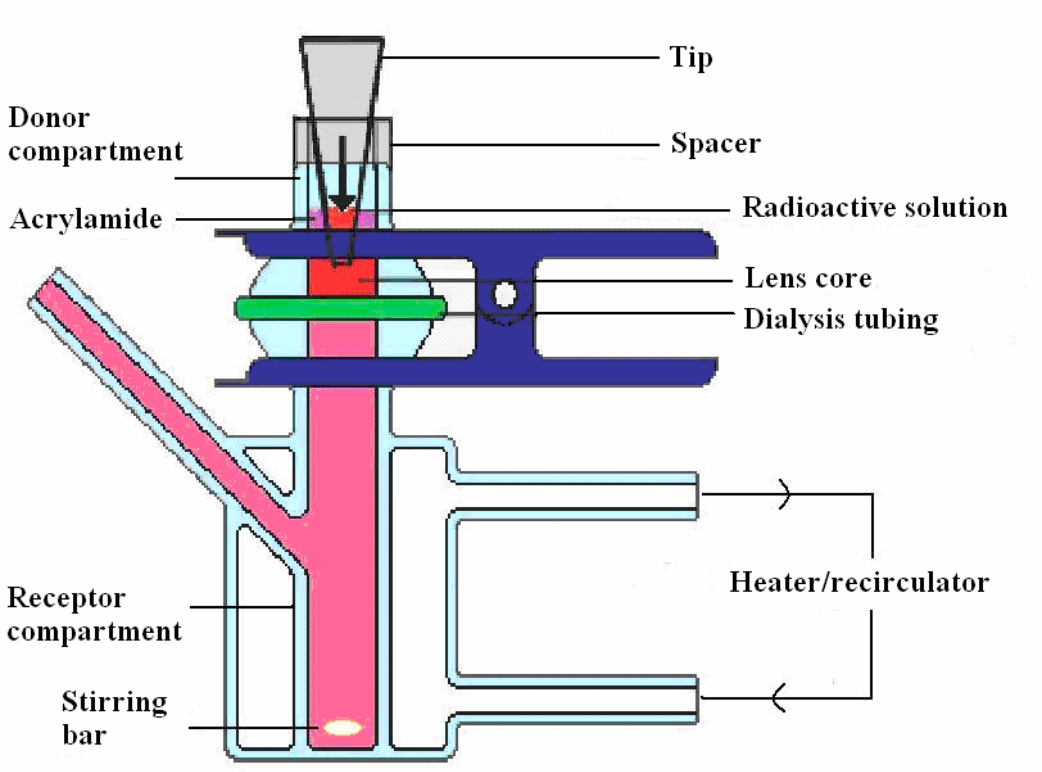

***Figure 2-1*: The diagram of the modified Franz Cell.**

2.2.2.2. Liquid Scintillation Counter

A liquid scintillation counter is an instrument commonly used to detect radioisotopes that emit low energy beta particles. A sample with an unknown amount of radioisotope is placed into an organic or aqueous solution, called a "counting cocktail". The electrons emitted from the radioisotope interact with the counting cocktail causing it to emit light. These flashes are detected and converted to amplified electrical pulses by a photomultiplier tube. The amount of isotope in the sample can then be measured.[29]

2.2.3. Procedures

2.2.3.1. Lens Tissue Specimens Preparation

To set up the Franz Cell procedure, pig and calf lenses were used. Pig/calf/human lenses were removed from the freezer and placed on a cold plate. The lens was partially thawed and then cored using a 5 mm internal diameter trephine incorporating a removable 5 mm diameter rod in the center (**Figure 2-2**).

Cortex parts were cut off the ends of the tissue specimens to generate a 2 mm thick nuclear lens plug, which was pushed into the donor compartment from the bottom (**Figure 2-2**). The donor compartment with the lens was stored at –20^{o}C.

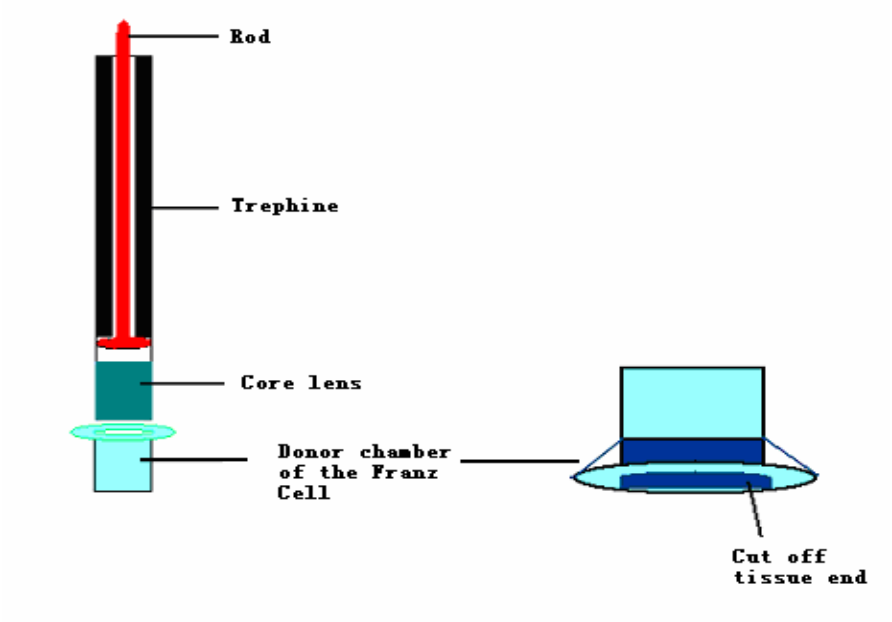

***Figure 2-2*: The diagram shows the lens sectioning process to obtain the core lens, and sample plug in donor chamber.**

2.2.3.2. Permeability Experiment

The receptor compartment of the diffusion cell was filled with 5 mL PBS buffer. Dialysis tubing was placed on top of the receptor compartment (exposed areas 0.2 cm^2). A clamp was then used to join the donor compartment (with tissue specimens) and receptor compartment. An Eppendorff tip was placed on the lens tissue surface, and pushed into the tissue (~0.1 mm). Poly-acrylamide was added and allowed to polymerise to stabilise the Eppendorff tip (**Figure 2-1**) and to seal any leaks.

Prior to commencement of the experiment, the system was equilibrated at 37^oC and the receptor chamber was stirred at 400 rpm using a magnetic stirrer (Industrial Equipment & Control Pty. Ltd., Australia). Tritiated water/PBS solution was then added to the Eppendorff tip. Aliquots (200 μL) of sample were withdrawn from the receptor compartment at predetermined times following 8 hours initialization. Each time an aliquot was removed, it was replaced by the same amount of PBS. Scintillation cocktail (5 mL; SIGMA-FLUOR Universal LSC cocktail, St. Louis, MO, USA) was then added to each 200 μL sample in a 7 mL scintillation vial (Packard Instrument Company INC, Meriden, CT, USA), and mixtures were counted in a liquid scintillation counter (Beckman LS 5000TD, Beckman Instruments, Fullerton, Calif., USA). Quenching for each sample was automatically corrected in the counter. Flux (J) values

across membranes were calculated by means of the following equation (**Equation 2-2**).

$$J = D/A \cdot t$$

where:
J = flux values ($dpm \cdot cm^{-2} \cdot min^{-1}$)
D = quantity of substance crossing membranes (dpm)
A = membrane area exposed (cm^2)
t = time of exposure (min)

***Equation 2-2*: The equation shows the calculation of flux values.**

2.3. Results and Discussion

Flux values (J) for tritiated water/PBS versus time for a young (24 years old) and an old (74 years old) human lens are shown in **Figure 2-3** (calculation with raw data see Appendix A). The mean steady state (after 20 hours) flux values for tritiated water/PBS solution diffusing through the different age lens tissue samples and across the dialysis tubing are shown in **Table 2-1**. The result shows that the diffusion did not significantly change in the nuclear region of the human lens with age.

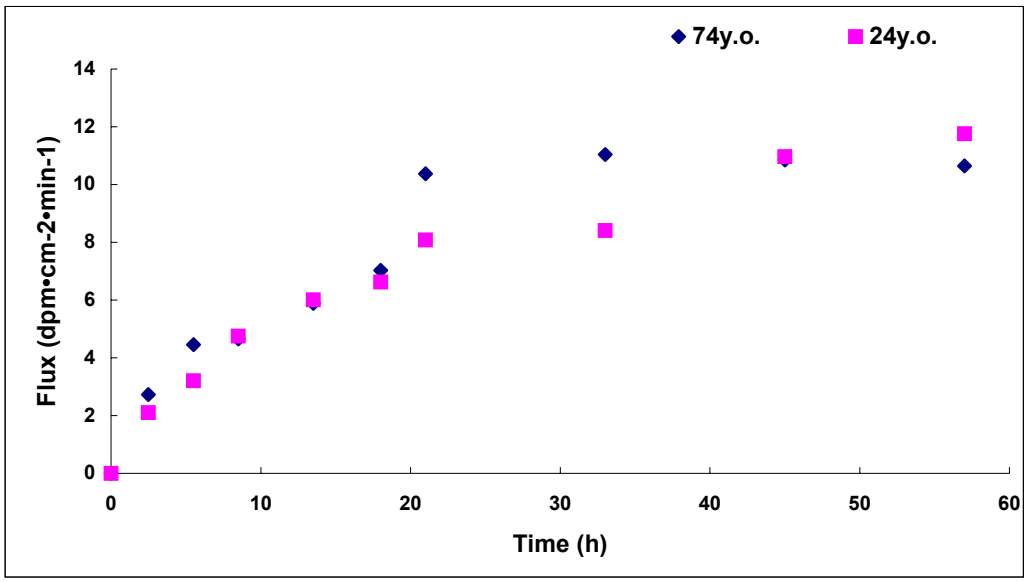

***Figure 2-3*: Flux values for tritiated water through two different human lens tissue samples (young 24 y.o. and old 74 y.o. lens) versus time.**
y.o.: years old

	24 y.o. Human lens	74 y.o. Human lens
Mean steady state fluxes (after 20 h)	**9.81+/-1.83 dpm•cm^{-2}•min^{-1}**	**10.73+/-0.29 dpm•cm^{-2}•min^{-1}**

***Table 2-1*: Mean (+/-STDEV) steady state flux values of tritiated water/PBS diffusion through the lens core of different ages. (n=4, collecting time at 21, 33, 45 and 57 hours)**

As mentioned previously, some studies have shown that many changes take place in the physical properties of the human lens with age (**1.2.3.**). The results of this study however showed that there was no significant change in diffusion between a young and an old human lens. However, these results may be influenced by several extraneous factors. The set up of the diffusion experiments is difficult and the results may not

reflect the diffusion property changes of the core lens correctly. Leaking was also a problem, even though several methods were used to avoid it. The diffusing solution may leak down the edge of the donor chamber, and produce similar diffusion rate results in each lens sample despite actual differences in diffusion rates in the lens tissues. It is very difficult to check for this factor. Measurable flux increases before 8 hours suggest that such leakage may have been taking place.

In order to confirm the results of this experiment, new methodologies need to be considered and designed. For example, the nucleus of a human lens can be incubated in artificial aqueous humor containing a low molecular weight radioactive isotope. The change in diffusion capability with age of human lens nuclei can be examined using a phosphorimager. Due to the time limitations of this study, insufficient time was available to plan a new experiment and to do trial experiments.

Two other factors, which the literature suggests may be important to lens barrier formation, were investigated as a part of the research project. Chapter 3 examines protein sulphydryl (SH) groups and oxygen consumption in the core lens and chapter 4 considers cholesterol compositional changes in the lens.

Chapter 3: Oxygen Consumption in the Lens

3.1. Introduction

3.1.1. Oxidative Stress

At middle age, a barrier forms in the human lens impeding the normal cycling of small molecules such as antioxidants.[16] This leads to an increase in average lifetime of spontaneously unstable molecules in the lens nucleus, which increases the chance of oxidation of proteins and post-translational modification of the lens crystallins. There is considerable evidence to link oxidative damage with the formation of age-related cataract, such as the oxidation of cysteine and methionine residues[30] in the nucleus. This oxidation[30] is found to be greatly increased in advanced cataract. Additionally, oxidation is also associated with a significant increase in the level of crystallins cross-linked by disulphide and other covalent bonds.[31, 32] The oxidation of sulphydryls in nuclear cataract is accompanied by a substantial loss of water-soluble (WS) protein.[33, 34] It is clear that a high level of reactive oxygen species (ROS) in the nuclear region contributes to ARNC development, [35] however, the source and identity of ROS have not been fully established.

Molecular oxygen (O_2) is the source of the ROS. The outer cortical region is one place where constant oxidative stress could be generated. The lens is permeable to numerous

small molecules, including O_2. ROS such as superoxide radical ($O_2^{\cdot -}$) and hydrogen peroxide (H_2O_2) have the capacity to enter the lens.[36] However, ROS may not be restricted in their diffusion into the center of the lens by the development of the barrier with age since they are small and highly diffusible. This is in contrast to glutathione and ascorbic acid. ROS may also be generated within the nucleus by oxygen-induced oxidation of reactive molecules such as ascorbic acid or 3-hydroxykynurenine. Oxygen is present in the center of lens, and can lead to oxidative damage.[37]

3.1.2. Oxygen Consumption in the Lens

As noted above, oxidation is a key factor of cataract. It may be important to keep a low level of oxygen in the lens in order to maintain the optical clarity.[38] However, a precise method to measure the oxygen levels in the lens has not been introduced until recently. The research done by McNulty et al. (**2004**) has shown the presence of oxygen in the lens, which exhibits a steep gradient from the outer parts of the lens into the lens center.[39] This suggests that the lens has at least one mechanism by which oxygen is consumed. Mitochondria, which are mainly present within the outer cortical region, appear to be the most likely entity to consume oxygen, thus helping to keep oxygen levels low in the nuclear region of the lens.[39] In order to fully understand the mechanism of oxygen consumption by mitochondria, it is necessary to review of their major features.

3.1.2.1. Mitochondria

Mitochondria are oval-shaped, membrane-bound intracellular organelles with dimensions of approximately 2 μm by 0.5 μm and are found in the cytoplasm of nearly all eukaryotic cells. They are especially abundant in cells, and parts of cells, that are associated with active processes such as synthesis.[40]

Structurally the mitochondria are comprised of a double-membrane, which generally can be described as a wrinkled bag packed inside of a larger unwrinkled bag. The mitochondria consist of four distinct sub-regions: the outer membrane, the inner membrane, the intermembrane space and the matrix that is located within the inner membrane (**Figure 3-1**).[41] The two membranes create distinct compartments within the organelle, and are themselves very different in structure and in function. The outer membrane is a relatively simple phospholipid bilayer, containing protein structures called porins, which render it permeable to molecules of about 10 kDa or less (e.g. ions, nutrients, ATP, ADP). The inner membrane is freely permeable only to oxygen, carbon dioxide and water. Its structure is highly complex, including all of the electron transport system, the ATP synthetase complex and transport proteins. It is also highly folded into cristae, which greatly increases the total surface area of the inner membrane.[42]

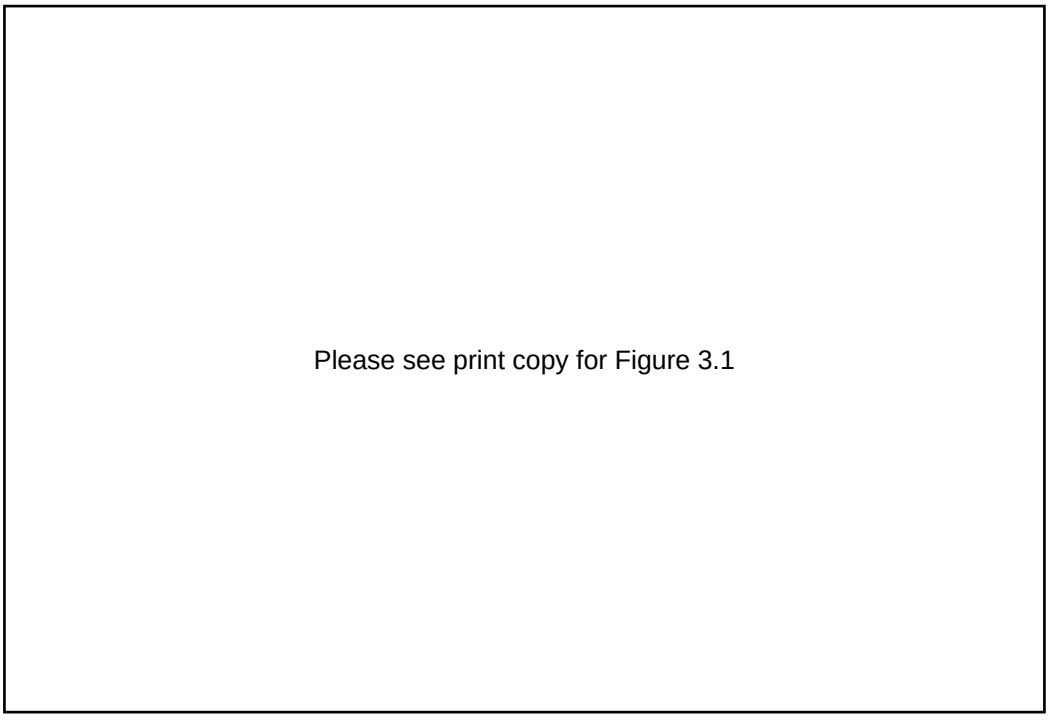

***Figure 3-1*: Mitochondria diagram showing the four distinct sub-regions (the outer membrane, the inner membrane, the intermembrane space and the matrix) and the localizations of respiratory processes occurring within the organelle.**[41]

3.1.2.2. Mitochondrial Oxygen Consumption

The mitochondrial membranes create two compartments. The intermembrane space, as implied, is the region between the inner and outer membrane. It has an important role in the primary function of mitochondria, which is oxidative phosphorylation. Oxidative phosphorylation occurs in the inner membrane and supplies the majority of the cellular energy produced under aerobic conditions. Oxidative phosphorylation combines hydrogen with oxygen to generate large amounts of ATP by passing through a series of intermediate electron carriers, a process called the electron transport chain (ETC). Components of the ETC system include complexes I, II, III and IV, plus two individual molecules, coenzyme Q and cytochrome C (**Figure 3-2**).[43] The electron

carriers nicotinamide adenine dinucleotide (NADH) and flavin adenine dinucleotide ($FADH_2$) derived mostly from the Krebs cycle in the matrix of the mitochondria, are oxidized to provide electrons for the ETC. As each electron passes through the ETC, a proton is forced from the matrix to the intermembrane space, creating a proton gradient. During the initial steps in processing, electrons from NADH go through complex I, while the electrons from $FADH_2$ pass through complex II. The reduced product of both complexes (complex I and II) is the same molecule, called coenzyme Q (CoQ). The electrons on CoQ are then passed through complex III to form the other reduced form of the molecule – cytochrome C (CytC), and are then transported to complex IV. Thus, O_2 is consumed in the process as electrons are passed along the ETC with the concomitant transfer of protons to form water. The proton gradient is then used by enzyme complex V (ATP synthase) to phosphorylate adenosine diphosphate (ADP), forming ATP.[44]

Mitochondria can consume oxygen through another process – proton leak, which is not associated with the manufacture of ATP. There is always a cycle of outward proton pumping and inward proton leak across the inner membrane, due to the inability of mitochondria to be completely impermeable to protons.[45, 46]

Therefore, there are two mechanisms of oxygen consumption in the inner membrane of mitochondria, one which is associated with the synthesis of ATP (coupled respiration) and the other one which is due to proton leak.

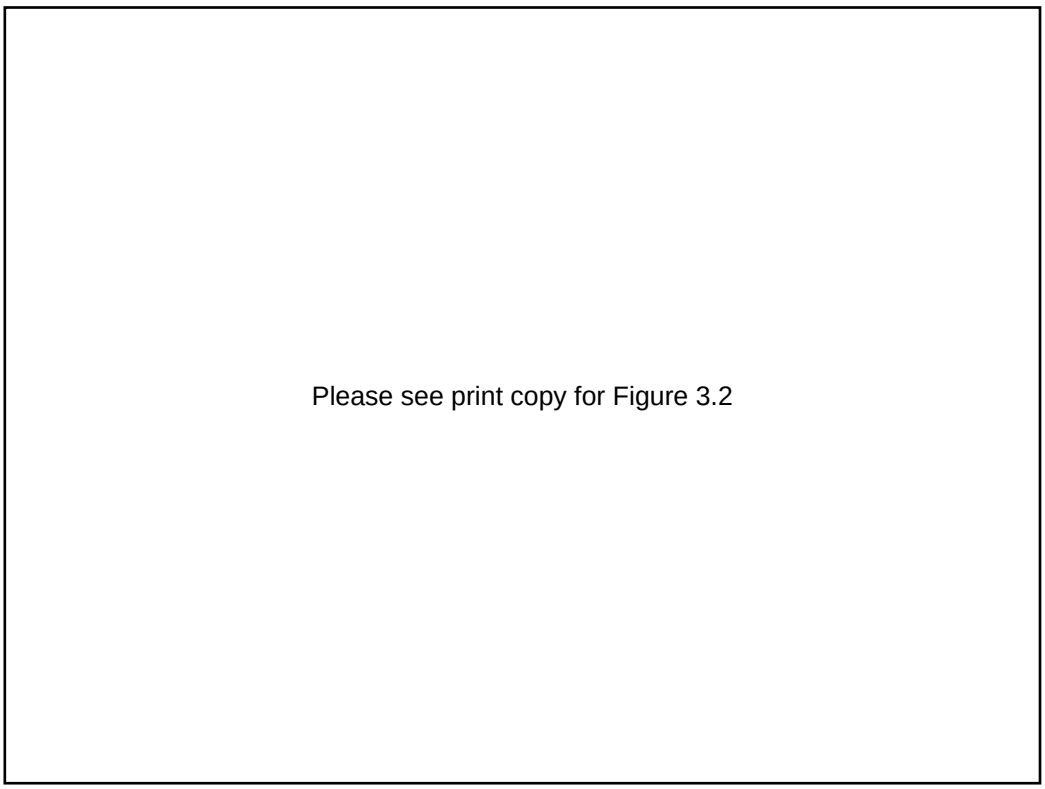

***Figure 3-2*: The electron transport chain. The system consists of an electron transport chain (I-IV) and an ATP synthase located in the inner membrane of the mitochondria. The red line shows the path of electrons, and the green lines show the paths of hydrogen ions (H^+). The movement of H^+ across the inner membrane at complexes I, III and IV creates a higher concentration on the intermembrane side of the inner membrane than on the matrix side. The energy released by H^+ returning to the matrix through ATP synthase provides the energy needed for ATP synthesis.**[75]

3.1.2.3. Non-mitochondrial Oxygen Consumption in the Lens

It is clear that mitochondria are the primary oxygen consumers in the lens, however, the core of the lens, which does not contain mitochondria, also shows oxygen consumption.[39] This non-mitochondrial oxygen consumption accounts for approximately 10% of total oxygen consumption in the lens,[38, 39] however, the basis for this mechanism is still not fully understood. Several hypotheses suggest that ascorbic acid and protein sulphydryl (PSH) groups play a role as potential non-mitochondrial

oxygen consumers in the lens. Ascorbic acid is considered to consume oxygen via a metal-catalysed reaction involving GSH, however, this is still not fully established.[22] GSH can also play a role in PSH oxygen consumption. This oxygen consuming process occurs due to oxidation of the sulphydryl groups to become a disulfide. Two moles of PSH react with one mole of O_2 to form a cystine residue (**Figure 3-3**). GSH can then reverse this reaction and convert the protein back to its reduced state.[39]

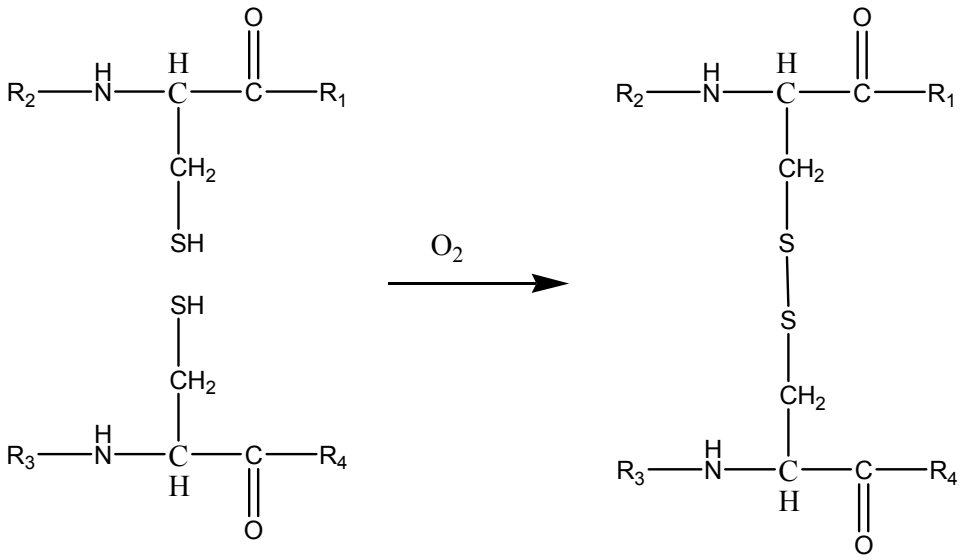

***Figure 3-3*: The oxidation of cysteine residues.**

With lens age, GSH levels decrease, by contrast, levels of PSH have not been observed to significantly decrease.[47] In the cataract lens, however, especially in the most advanced case (type IV), the level of PSH shows a significant difference between the nuclear and cortical regions. The nucleus contains a much lower value of PSH in comparison with the cortex. By contrast, in the normal lens, the values of PSH are very similar between the nucleus and the cortex. It is believed that PSH oxidation plays a

major role in the formation of high molecular mass (HMM) aggregation in the lens, which is related to the formation of cataracts.[48] This study aims to determine how oxygen is consumed by PSH.

3.1.3. Oxygen Analyzer – Clark (pO_2) Electrode

Electrochemical oxygen analyzers are based on electrochemical reduction of O_2 at a negatively polarized electrode. The Clark electrode (**Figure 3-4**) consists of an anode and cathode covered by a layer of electrolyte solution. It is covered at the tip by a semi-permeable membrane, normally a polypropylene or Teflon membrane, which is permeable to gases, but not to contaminants or reducible ions in the sample. The Clark electrode measures partial pressure of oxygen (pO_2) amperometically. That is, the electrode produces a current, which is directly proportional to the pO_2 diffusing through the membrane in a given time. The Silver/Silver Chloride (Ag/AgCl) anode provides electrons for the cathode reaction (**Equation 3-1**). Oxygen molecules diffuse through the semi-permeable membrane and the reduction of O_2 then occurs at the cathode by combining O_2 with the electrons from the anode (**Equation 3-1**). The pO_2 channel measures this flow of electrons and the resulting micro-voltage is displayed as pO_2. The Clark electrode can also be used to measure pO_2 over time (i.e. O_2 consumption). This can be done by immersing the sample in a solution with a known level of oxygen in a closed respiratory chamber. The pO_2 is reported over time when the electrode is connected to a dissolved oxygen meter.[49]

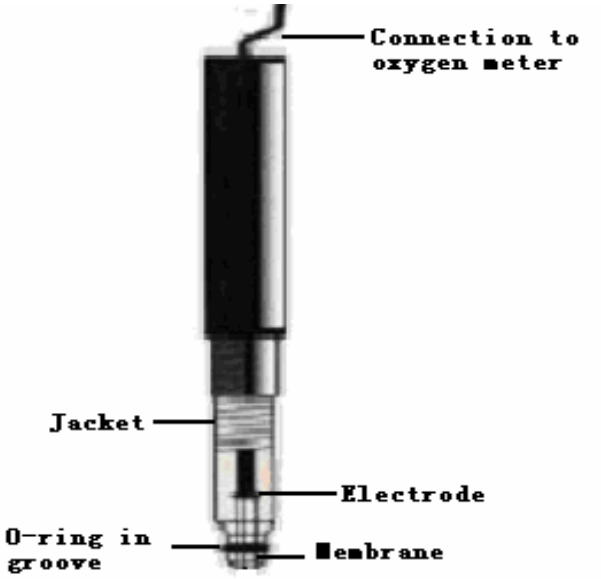

***Figure 3-4*: Clarke-type oxygen electrode. O_2 diffuses to the electron tip through the membrane and redox reactions occur, resulting in a current, which can be correlated to the partial pressure of oxygen.**

$$\textbf{Ag anode:}\quad 4Ag + 4Cl \longrightarrow 4AgCl + 4e^-$$

$$\textbf{Pt cathode:}\quad O_2 + 4H^+ + 4e^- \longrightarrow 2H_2O$$

***Equation 3-1*: The reactions on the Ag anode and Pt cathode of Clark-type oxygen electrode. The electrons are provided by the Ag anode for oxygen reduction on the cathode.**

3.1.4. Research Aims

Protein SH groups could potentially be the primary oxygen consumers in the nuclear region of the lens. This study aimed to investigate the role of PSH in maintaining a low concentration of oxygen in the core lens by modifying the protein SH groups in lens crystallins.

3.2. Experimental

3.2.1. Chemicals and Solutions

All chemicals used were from Sigma-Aldrich Chemical Company (St. Louis, MO, USA). All solutions in the experimental work were prepared using Milli-Q water purified to 18.2 MΩ cm^{-1}.

HEPES Tissue Buffer

The buffer contained 120 mM KCl, 5 mM KH_2PO_4, 3 mM HEPES, 1 mM EDTA, 1 mM $MgCl_2$ (pH 7.2).

Urea Tissue Buffer

The buffer contained 8 mM urea, 120 mM KCl, 5 mM KH_2PO_4, 3 mM HEPES, 1 mM EDTA, 1 mM $MgCl_2$ (pH 7.2).

Bovine Serum Albumin (BSA) Standards

BSA standards were prepared using the attached table in the BCA Assay Kit (PIERCE, IL, USA), as a guide, to prepare the following concentrations: 2000 μg/mL, 1500 μg/mL, 1000 μg/mL, 750 μg/mL, 500 μg/mL, 250 μg/mL, 125 μg/mL, 25 μg/mL and 0 μg/mL. Samples were stored at –20^{o}C until used.

BCA Working Reagent (WR)

BCA Reagent A (sodium carbonate, sodium bicarbonate, bicinchoninic acid and sodium tartrate in 0.1 M sodium hydroxide) (15 mL) and BCA reagent B (4% w/v cupric sulfate) (0.3 mL) were combined to form the WR.

3.2.2. Biological Materials

Bovine Lenses

See section **2.2.1.1.**.

Sectioning of Bovine Lenses

Bovine lenses were sectioned into nuclear and cortical regions using a 5 mm diameter cork-borer. Both ends (~1.5 mm) of the core of the lenses were removed with a razor blade. The sections were then placed into a tissue culture dish and weighed. This procedure was done initially before the PSH oxygen consumption experiment.

3.2.3. General Equipment

Oxygen Electrode

O_2 consumption was determined using a Strathkelvin (Glasgow, UK) 1302 polarographic O_2 electrode in an electrode holder submerged in an RC 350 glass chamber and attached to a Strathkelvin 781 dissolved O_2 meter. The output from the electrode was fed to an ADI Instruments (Sydney, Australia) coupled Maclab data acquisition system and connected to a Macintosh Power PC (7200/120).

Sample Preparation

Centrifuge: the centrifuge used in the experimental methods was a Beckman Allegra 21R Centrifuge, which used either an F-0850 (for isolation of PSH determination) or F-3602 (for removal of insoluble proteins) rotor. UV-Visible Spectrophotometer: a Shimadzu UV-265 UV-visible recording spectrophotometer was used for the PSH measurements. Microplate Reader: a SpectraMax 250 (Biolab Instrument Servicing, Australia) spectrophotometric microplate reader was used for protein assay experiments. Homogenizer: bovine lenses were homogenized using a pre-cooled ~20 mL glass-teflon tissue homogenizer (Clearance: 0.18-0.23 mm, Glas-Col, IN, USA).

3.2.4. PSH and Protein Assay

The PSH value in homogenates of lens cores was determined using a modified method

of that described by Sedlak and Linsay (**1968**),[50] as used by Berry and Truscott (**2001**)[51].

To determine the PSH content of the sample, 1 mL of lens core homogenate (~100 mg/mL wet weight) was added to the same volume of 10% TCA (trichloroacetic acid) containing 0.01 M EDTA (TCA/EDTA solution) in a centrifuge tube. The solution was then flushed with N_2 and centrifuged at 3000 g for 10 minutes at 4^{o}C. This process was repeated on the pellet with a further 1 mL of the TCA/EDTA solution, and then washed again with 1 mL of cold Milli-Q water, which was then discarded. The pellet was dissolved in 1 mL of 0.2 M ammonium bicarbonate containing 8 M urea. The resulting solution (solution A) was used for the testing of PSH and protein concentration.

PSH Assay

125 μL of solution A was added to the dilution buffer 1.975 mL of 0.5% SDS solution, 375 μL of 0.2 M, pH 8.2 Tris-HCl solution.

The absorbance of the initial solution was measured at 412 nm. Next, 25 μL of DTNB (5,5'-Dithio-bis(2-nitrobenzoic acid)) buffer (0.01 M in methanol) was added. This solution was allowed to stand for 30 minutes at room temperature with occasional shaking after which the absorbance was measured at 412 nm. PSH concentration is determined through the increase in the absorbance at 412 nm with reference to a standard curve covering the range of 0-150 μM cysteine.

N.B.: SH groups readily oxidize at pH 7-9 but only slowly at an acidic pH, therefore, once the pH has been adjusted upwards, a measurement should be performed immediately. This is important when using solution A in the PSH assay.

BCA Protein Assay

Standards or protein samples (25 µL) were pipetted into microplate wells. 200 µL aliquots of working reagent (WR) were added to each well, and the plate was mixed thoroughly for ~30 seconds. The plate was covered and incubated at 37^{o}C for 30 minutes. The absorbances of the cooled solutions were measured at 562 nm on the plate reader. A standard curve was prepared by plotting the absorbance against BSA concentrations (µg/mL), and the standard curve was used to calculate the protein concentration of each sample.

Considering that ascorbic acid from the lens homogenate may interfere in the BCA protein assay, the Coomassie protein assay (protocol see Appendix C) was therefore used to confirm the result. The comparison of results of each assay showed no differences. Ascorbic acid does not appear to interfere with the result of the BCA protein assay.

3.2.5. Measurements of PSH Oxygen Consumption

3.2.5.1. O_2 Consumption

The measurement of oxygen consumption was achieved by putting samples in a closed glass chamber, which was magnetically stirred at ~500 rpm (**Figure 3-5**) to maintain a homogeneous dissolved-O_2 concentration. All O_2 consumption measurements were performed at 37^{o}C. For each measurement, 1 mL of sample was used and oxygen consumption was measured following thermal equilibration of ~8 minutes.

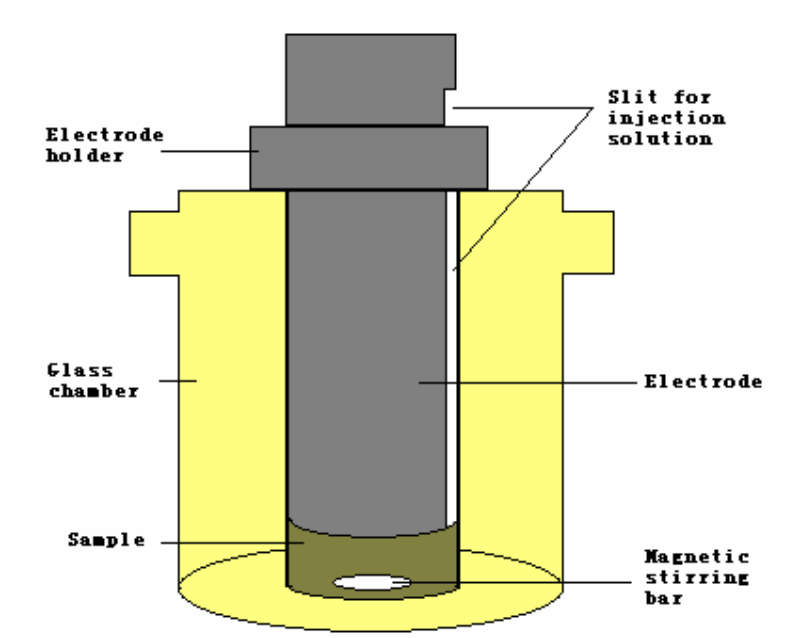

***Figure 3-5*: The glass chamber containing the electrode and the electrode holder. The electrode is connected to the oxygen meter.**

Prior to each measurement, the oxygen electrode was calibrated with air-saturated water (pO_2 of ~150 mmHg), and also a solution with excess sodium dithionite (to achieve a zero pO_2). All oxygen consumption measurements were calculated as the rate of decrease in O_2 concentration assuming an initial O_2 concentration of 214.4 nmole/mL (Henry's Law).

3.2.5.2. Non-mitochondrial Oxygen Consumption

Iodoacetic acid (IAA) was used to partially block the number of PSH groups available for reacting with oxygen. IAA reacts with the PSH group of the cysteine residue forming carboxymethyl cysteine (**Figure 3-6**).

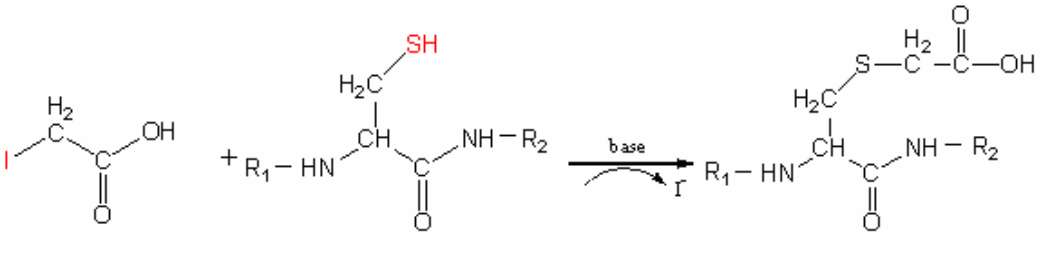

***Figure 3-6*: Carboxymethylation of cysteine residues with the alkylation agent iodoacetic acid (IAA).**

A batch of lens cores (for preparation see section **3.2.2.**) was homogenized in the HEPES or urea tissue buffer (**3.2.1.**) at ~100 mg/mL wet weight. The homogenate was then separated into 2 mL aliquots, which were labeled. IAA solution was prepared by dissolving IAA in 1 M NaOH at 0.1 g/mL. In order to obtain various PSH/protein ratios (mole/mole), different amounts of IAA were added to samples to block PSH. Sample 1, using each tissue buffer, was not treated with IAA. Samples 2-6, using HEPES tissue buffer, were treated with 8 µL, 16 µL, 32 µL, 64 µL and 128 µL of the IAA solution. In separate experiments, 64 µL and 256 µL IAA were also added into samples using the urea buffer. All samples were incubated at room temperature for 30

minutes and were snap-frozen in liquid nitrogen and stored at –20°C until used. A sample was thawed each time and O_2 consumption was measured for 25 minutes following thermal equilibration using 1 mL of sample. The other half was used for PSH and protein assay to determine the PSH/protein ratio in the sample. Oxygen consumption for each sample (μmole/g/hr) was then plotted against its corresponding PSH concentration.

3.3. Results and Discussion

3.3.1. The Effect of Freezing

The effect of freezing on the loss of PSH in solution A (**3.2.4.**) was studied. The PSH concentration in protein of solution A that had been frozen 48 hours in a –20°C freezer was compared with the PSH concentration of fresh solution A. The results show a notable difference, with nearly half of the PSH lost in the frozen sample (**Figure 3-7**). This may happen due to the conversion of ammonium bicarbonate to ammonia with time, which results in the increase of the pH value of the solution. The SH group readily oxidized at pH 7-9. Therefore, the PSH and Protein assay was performed immediately after solution A was made in all O_2 consumption studies.

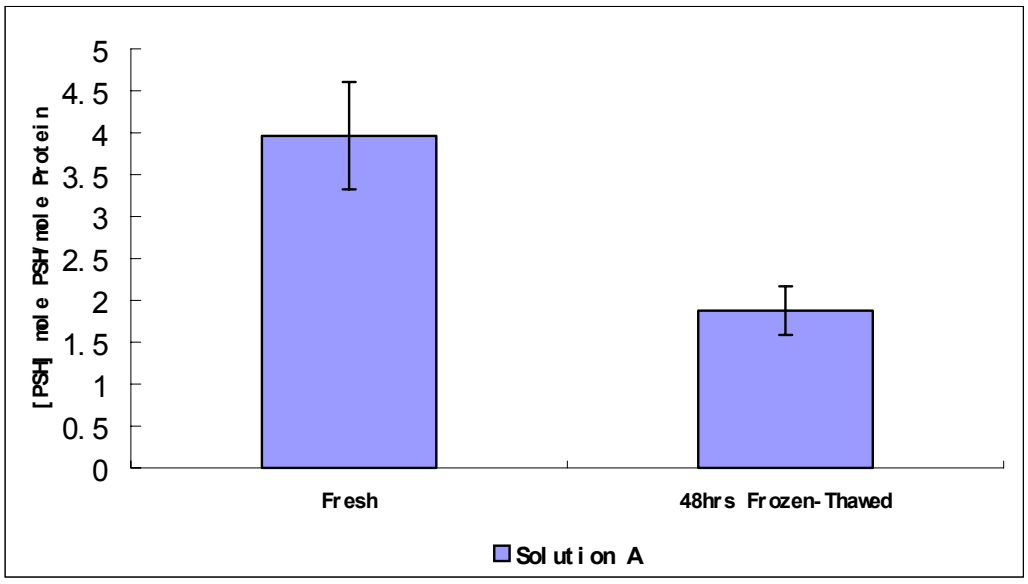

***Figure 3-7*: The effect of freezing on [PSH] (mole PSH/mole Protein) in solution A.**

3.3.2. Protein Sulphydryl in the Lens Core as Potential Oxygen Consumer

There are no organelles present in the lens core, however, protein SH groups are abundant. The PSH oxidation therefore is considered responsible for oxygen consumption in the nuclear region. The role of PSH in the lens core as a potential non-mitochondrial O_2 consumer was studied by chemically blocking a proportion of the PSH groups using IAA. Different ratios of PSH/protein were examined for O_2 consumption.

Oxygen consumption values versus PSH concentrations using both HEPES buffer and urea buffer are shown in **Figure 3-8**. The 8 M urea was used to unfold the protein and

therefore to expose all PSH groups. It was observed that in general, oxygen consumption values decreased as the PSH/protein ratio fell. The variation of the PSH/protein ratio of the two samples using urea and no urea (circled in **Figure 3-8**) without added IAA may demonstrate that the urea can unfold the protein structure, to expose buried protein SH groups. The previously reported PSH/protein ratio (mole/mole) in the nucleus of bovine lens using 8 M urea buffer is ~4.5,[51] is in good agreement with the data below. These data suggest that, on average, one sulphydryl group per mole of protein in the lens nucleus is buried.

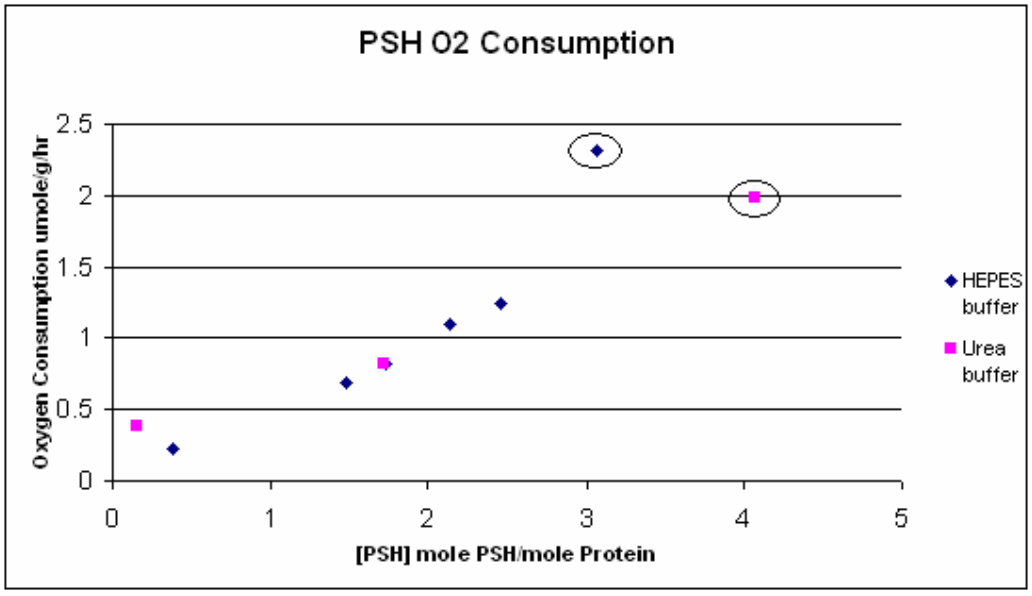

***Figure 3-8*: The relationship between PSH in the lens core and O_2 consumption. O_2 consumption rates were measured at 37°C in a closed chamber assuming an initial oxygen concentration of 214.4 nmole/mL (~150 mmHg). Units are given as μmole O_2 per**

hour per gram lens core. ~100 mg/mL (wet weight) were used for each measurement.

It is also clear that even with the PSH/protein ratio close to zero, O_2 consumption still could be observed, especially if the sample is in a urea buffer. It reflects that other residues (e.g. protein methionine) or compounds such as ascorbic acid may be consuming O_2 at a slow rate. The results, however, support the idea of PSH as a primary oxygen consumer in the lens center.

3.3.3. Future Work

In this study, PSH groups in lens nucleus proteins were determined to act as oxygen consumers. In future studies, the experiments could be repeated to mimic the real lens environment by using a low O_2 gas (1% Oxygen in Nitrogen), to investigate the role of PSH in maintaining a low concentration of oxygen in the center of the lens.

3.4. Conclusions

The lens core contains crystallins that are unusually rich in the PSH groups. This, at first, may seem peculiar because cysteine residues are known to be subject to both oxidation and chemical modification. This poses an apparent conundrum because maintenance of protein structure is important for lens transparency. The results of this study suggest a reason why crystallins in the nucleus are rich in PSH. This could be to serve as a reserve system for eliminating any excess O_2 that diffuses past the

mitochondria in the cortex. The lens therefore appears to have two systems for maintaining low O_2 level in the nuclear region. PSH serves as a secondary internal system for maintaining a low concentration of O_2 in the lens, with mitochondria being the primary outer system. If PSH groups are oxidised by O_2, GSH can re-reduce them.

Chapter 4: Cholesterol Quantification

4.1. Introduction

4.1.1. Membrane Lipids

Membrane lipids are comprised of a polar hydrophilic head group and a non-polar hydrophobic hydrocarbon tail, and play an essential role in structuring and regulating cellular membrane function (**Figure 4-1**).[52] The main components of a membrane are phospholipids and cholesterol. Phospholipids (**Figure 4-1**) are the most abundant and are the major structural lipids in membranes. They are able to form membrane lipid bilayers due to their amphipathic nature. Their hydrophilic (water loving) end interacts with water and orients towards the extracellular space or cytoplasm, whereas their hydrophobic (water fearing) end orients towards the interior of the membrane. The strongly opposed preference of the "head" (hydrophilic) and "tail" (hydrophobic) areas of membrane lipids results in the formation of lipid bilayers in aqueous media.[52] However, the focus of this study is the other major component of the cell membrane – cholesterol.

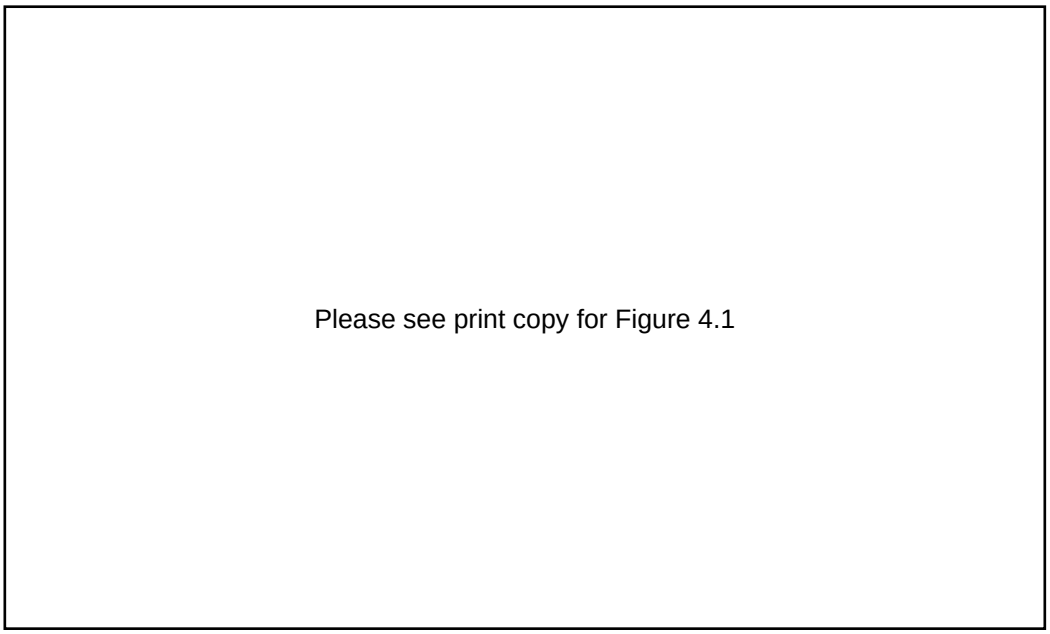

***Figure 4-1*: Structure of a cell membrane showing the interaction between membrane proteins and membrane lipids such as cholesterol and phospholipids.**[76]

4.1.2. Cholesterol

Cholesterol is an important biological molecule that has a role in membrane structure. It lies perpendicular to the plane of the membrane bilayers with its hydroxy group interacting with the polar head group of phospholipid (**Figure 4-1**).[53] Cholesterol acts as both a major structural component of the cell membrane and a precursor for other sterol lipids. Cholesterol, along with glycerophospholipids and sphingomyelins, serves as an important component of the cell membrane by modulating its physical properties such as fluidity.[53, 3]

Cholesterol, as shown in **Figure 4-2**, is composed of four fused carbon rings, an aliphatic side chain at C17 on ring D, methyl groups at C10 and C13, a double bond in ring B, and hydroxyl group on C3. The presence of the polar hydroxyl group ensures

that cholesterol is able to orient correctly in the membrane.[53]

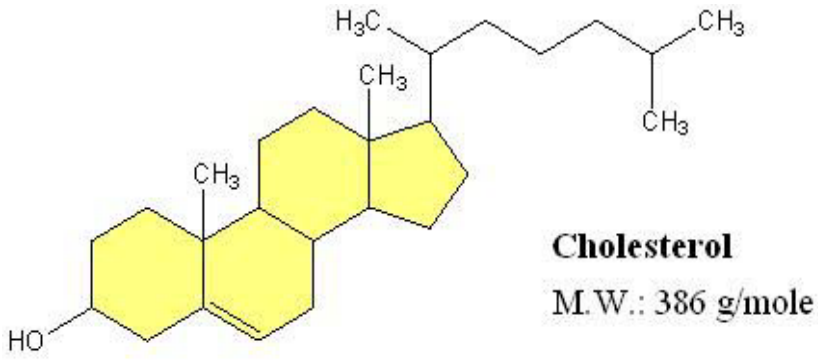

***Figure 4-2*: The structure of cholesterol.**

4.1.3. Cholesterol in the Lens

In the lens, fibre cells lack intracellular organelles, thus all cholesterol in the tissue is located in plasma membranes.[54] Human lens membranes contain the highest cholesterol content of any known biological membranes.[54, 55]

Cholesterol concentration shows a significant change with age, and also differs in different regions of the lens with a higher level of cholesterol in the nuclear region than that in the cortical region.[55] Therefore, the age-related change of cholesterol concentration may be an important indicator of the changing properties of the lens with age, and may also contribute to the age-related increase in human lens stiffness.[5]

4.1.4. Cholesterol and Aging of the Lens

Presbyopia is a major pathology of the human lens, which is associated with age. Presbyopia, the loss of focusing ability for nearby objects at middle age, can be measured via the steady loss of accommodative power with age.[56] Accommodative power is the ability of the lens to physically change shape in order to focus light on the retina. It occurs through contraction of the ciliary muscle, which releases tension on the zonules and leads to the moulding of the lens into the accommodated state by the lens capsule (**Figure 4-3**).[57]

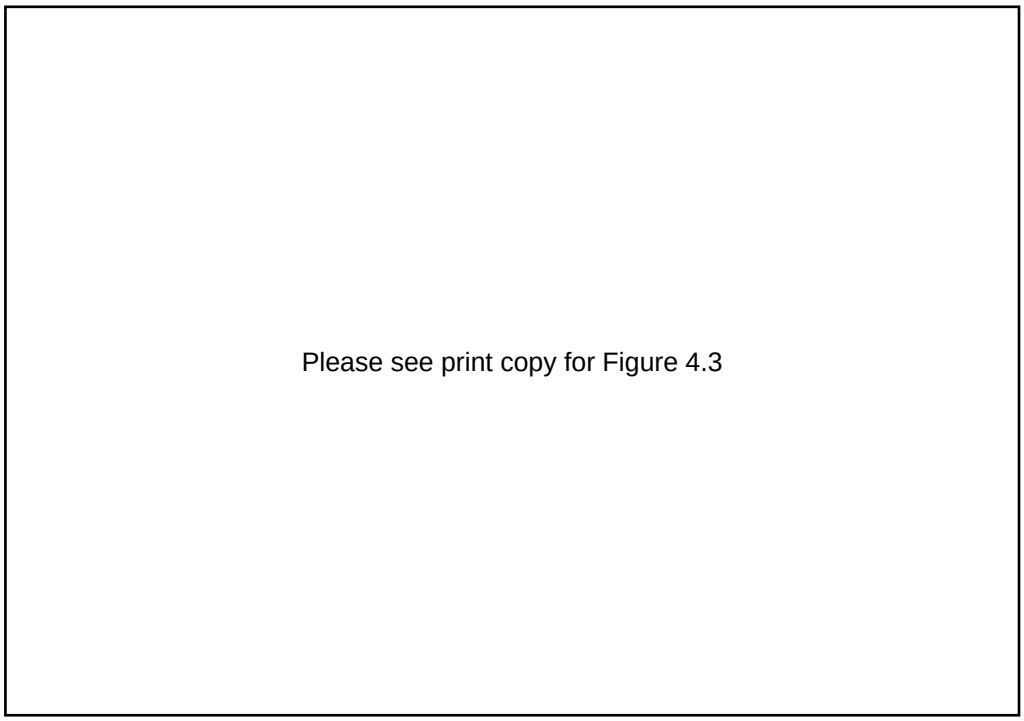

***Figure 4-3*: Diagram illustrating the process of accommodation. The lens is flatter for distant (*left*) and rounder for close vision (*right*).**[77]

The primary reason suggested for the loss of accommodation power with age is the enormous increase of the stiffness in the lens, especially in the nuclear region. Studies

have found that the nucleus of the lens has an approximately 450-fold increase in stiffness with age.[5] The physical properties of the lens are dependent upon the capsule, crystallins, the cytoskeleton, and also the fibre cell membranes themselves. Cholesterol and phospholipid, as major components of the cell membrane may play a decisive role in the physical properties of the cell membrane, such as permeability and fluidity. Since the fibre cells are locked together via cellular junctions, shape change of the lens must involve change to the shape of individual fibre cells. Recent studies have suggested that the increase in cholesterol content leads to increased membrane rigidity.[58, 59] This may be related to the increase in stiffness in the lens with age.

As with unsaturated lipids, cholesterol is prone to oxidation in the presence of reactive oxygen species. Some researchers have found that cholesterol oxides accumulate in cataract lenses, and suggest that cholesterol may be one possible target of oxidation in the lens, and in this way, may lead to the onset of cataract.[60] Additionally, the presence of high levels of cholesterol and its oxidized derivatives in the nuclear region may influence the association of proteins with nuclear membranes. The onset of cataract involves massive binding of proteins to the fibre cell plasma membrane.[61]

Therefore, changes in the content of cholesterol in cell membranes with age were investigated in this study.

4.1.5. Mass Spectrometry

A mass spectrometer can be used to provide analyses of a broad range of biological species from small molecules to large biological complexes. A mass spectrometer creates charged ions from molecules, and then analyses those ions to provide information about the molecular weight of the compound and its chemical structure. There are various types of mass spectrometers, however, all mass spectrometers consist of three distinct regions: an ionization source, mass analyzer and detector (**Figure 4-4**). Normally, these three regions are all maintained under high vacuum to give the ions a reasonable chance of traveling from one end of the instrument to the other without hindrance from air molecules.[62]

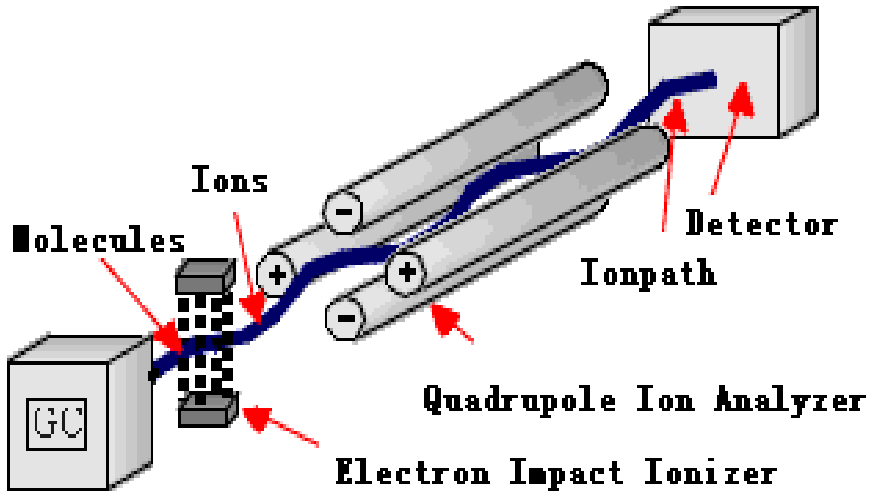

***Figure 4-4*: The basic structure of a mass spectrometer shows the three distinct parts, ionization source, mass analyzer and detector.**

Ionization Sources (Ionizer)

An ionization source is where samples are volatilized and ionized prior to detection in the mass analyzer. The samples undergoing investigation are first introduced into the ionization source of mass spectrometer. Many ionization methods are used for mass spectrometry, and the method chosen depends on the type and complexity of the sample as well as the desired degree of excitation of the analyte molecules during the ionization process.[62] The ionization methods used for the majority of biochemical analyses are electrospray ionization (ESI) and matrix assisted laser desorption ionization (MALDI). In this study, electron impact ionization (EI ionization) was chosen due to its energetic fragmentation of the analyte molecules. This provides the capability for working directly using a dilute solution, and is suitable for use of polar solvent[63] as $CHCl_3$ or MeOH, which were both used to dissolve cholesterol in this study.

EI Ionization

In EI ionization, electrons are produced on one side of the source from a heated rhenium or tungsten filament. The electrons are then energized by acceleration through an electric field to form a high-energy electron beam, which bombards the gas molecules. An electron, which strikes a molecule, may impart enough energy to remove another electron from that molecule (**Equation 4-1**).[63]

$$M + e^- (70eV) \longrightarrow M^+ + 2e^-$$

***Equation 4-1*: The equation summarises molecular ionization by EI.**

EI ionization usually produces singly charged ions containing one unpaired electron. A charged molecule, which remains intact, is called the molecular ion. However, energy imparted by the electron impact can leave a molecular ion with excess energy. If this energy is sufficient, the molecular ions can break into small pieces (fragments), to produce lower mass ions and neutral species.[63]

Mass Analyzer

The main function of the mass analyzer is to separate the ions, which are extracted into the analyzer region from the ionization source of the mass spectrometer, according to their mass (m) to charge (z) (m/z) ratios. There are a number of mass analyzers available. The quadrupole ion analyzer is one of the most popular mass analyzers.[64]

Quadrupole Mass Analyzers

The quadrupole mass analyzer consists of four parallel metal rods to which are applied both a DC voltage and a radio frequency oscillation (Rf) voltage as shown in **Figure 4-5**.[64] Molecular ions and fragment ions are accelerated by manipulation of these parameters to facilitate passage of the charged particles through the mass spectrometer.

Uncharged molecules and fragments are pumped away. The quadrupole mass analyzer uses positive (+) and negative (-) voltages to control the path of the ions. Ions travel down the path based on their mass to charge ratio (m/z). Mass separation in quadrupole mass analyzer is achieved by inducing oscillations in ions using a hyperbolic electric field. Ions of different m/z ratios travel in different paths at a particular DC and Rf voltage, and ions can therefore be separated and specially selected.[64]

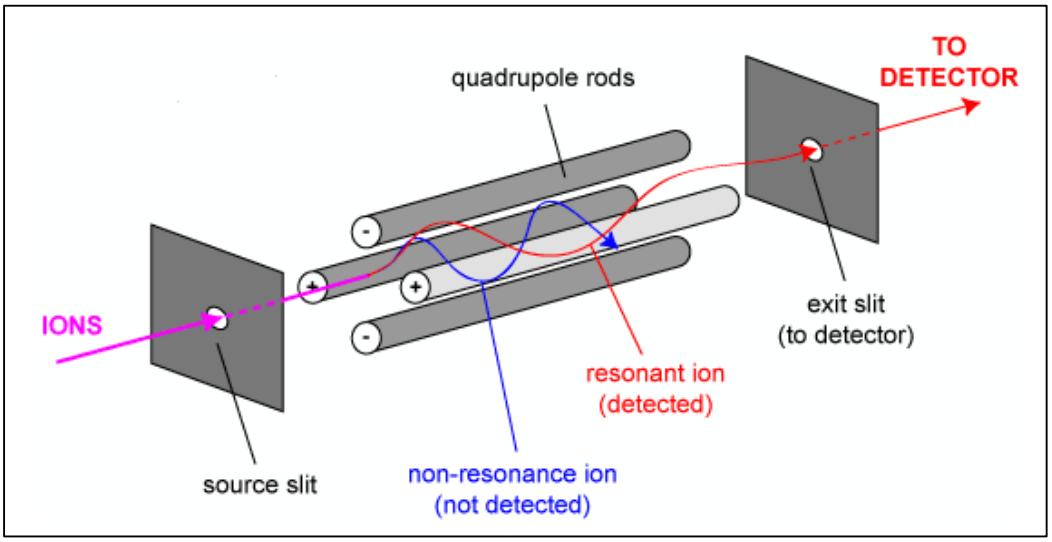

***Figure 4-5*: A quadrupole mass analyser.**

Detector

The detector monitors the separated ion current, amplifies it, and the signal is then transmitted to a data system where it is recorded in the form of an m/z spectrum. The m/z values of the ions are plotted against their intensities to show the number of components in the sample, the molecular weight of each component, and the relative

abundance of the various components in the sample.[62]

4.1.6. Project Aims

The aims of this project were to:

- Develop a rapid method for the quantification of cholesterol using direct insertion mass spectrometry with deuterated cholesterol as an internal standard.
- Compare the cholesterol levels in bovine, porcine, ovine, chicken and human lenses using the newly developed quantification method.
- Investigate cholesterol content in the human lens with age.

4.2. Experimental

4.2.1. Chemicals and Materials

All chemicals used were from Sigma-Aldrich Chemical Company (St. Louis, MO, USA), except solvents used in lipid extraction procedure, which were from Crown Scientific (Sydney, Australia), standard cholesterol (Prolabo Inc., Paris, France) and deuterated (2,2,3,4,4,6-D6) cholesterol (Cambridge Isotope Laboratories, Inc. MA, USA). All solutions in the experimental work were prepared using Milli-Q water purified to 18.2 MΩ cm^{-1}. All lenses were obtained and treated as described in section **2.2.1.1.**, and some animal lens lipid extracts were kindly supplied by Jane Deeley.

4.2.2. Lipid Extraction

Lens lipids were extracted using the Folch method[65] with minor modification. In the first step, lenses were frozen under liquid nitrogen in a glass centrifuge tube, and crushed using a pestle. Then, chloroform-methanol mixture (2:1 v/v) was added and the lens homogenized at a ratio of 20:1 solvent to tissue (v/w). The centrifuge tube containing the lens homogenates was placed in a tube rotator (Ratek RSM7, RATEK Instruments PTY. LTD., VIC, Australia) over night at 4^{o}C. The crude extract was then mixed with 1 M sulfuric acid (1:1 v/v), and the mixture was separated into two phases by centrifugation at 400 *g* for 10 minutes (Beckman Allegra 21R, Beckman Coulter Inc., CA, USA). The organic layer was collected and the same amount of chloroform-methanol mixture was added to the aqueous layer and centrifuged as before. Both of the organic layers were combined and mixed with sulfuric acid (1 M) (1:1 v/v). The mixture was centrifuged under the same condition. The organic layer was retained, and anhydrous sodium sulfate was added (~50 mg) for ~5 minutes before removal via filtration through silane-treated glass wool. The extract was concentrated to dryness by vacuum distillation of the solvents using a stream of dry nitrogen and the residues were then re-dissolved in MeOH:$CHCl_3$ (1:1 v/v, Density 1.14).

NB: All solvents used in this procedure were HPLC grade and contained butylated hydroxytoluene (0.01% w/v).

4.2.3. DI/EI Mass Spectrometry

This study attempted to establish a method to quantify cholesterol in lipid extracts, by using direct insertion (DI)/EI mass spectrometry. In DI/EI mass spectrometry, the probe containing the dried sample is heated e.g. at rate of 150^{o}C/min from 50^{o}C to 300^{o}C and the source is maintained at the temperature of 250^{o}C to ensure rapid evaporation. DI/EI analysis therefore provides mass spectra for all of the analytes present in the sample that are thermally stable and sufficiently volatile to be vaporized into the ion source. To be suitable for DI/EI quantification, it was crucial that all the major ions that appeared on the spectrum were from cholesterol only. In a test run of a lipid extract using DI/EI mass spectrometry, the spectrum (**Figure 4-6)**, showed that the only ions detected in the mass range (m/z 260-425) were those ions derived from cholesterol. There were no interfering peaks from other lipids in the extract, such as those from fatty acids and phospholipids.

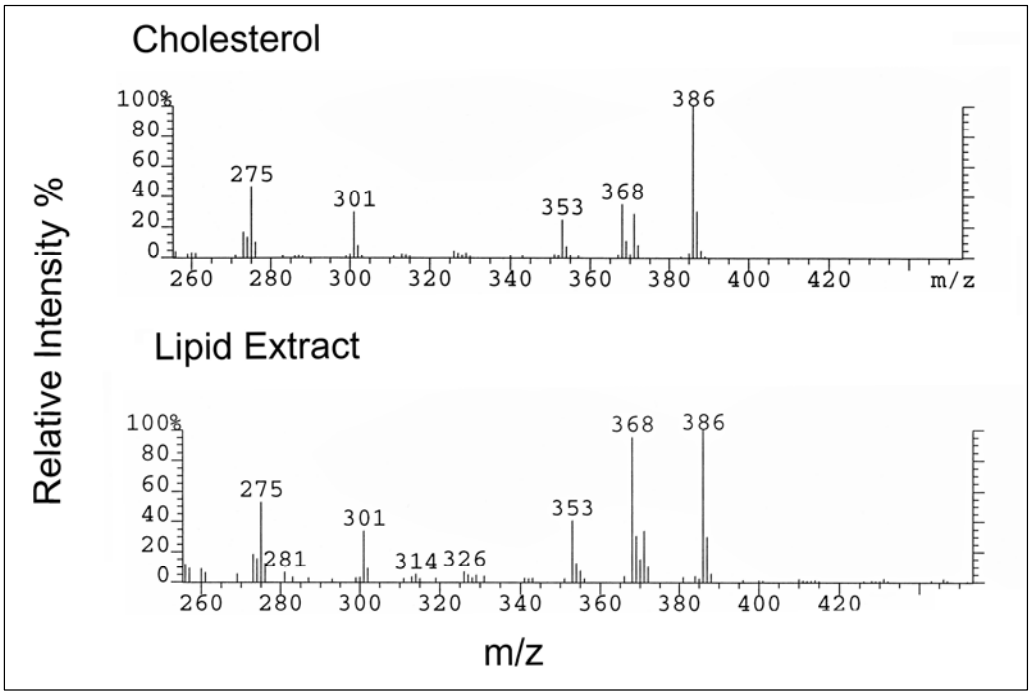

***Figure 4-6*: A comparison of the database spectrum for cholesterol (*upper figure*) and the spectrum of a lipid extract from a human lens (*lower figure*).**

4.2.4. Internal Standard

For cholesterol quantification, an appropriate internal standard was required which must behave similarly to cholesterol but be of different mass. Commercial deuterated cholesterol ($C_{27}D_6H_{40}O$) was chosen since it satisfies all the requirements as an internal standard. A mass spectrum of deuterated cholesterol is shown in **Figure 4-7** (m/z 330-405).

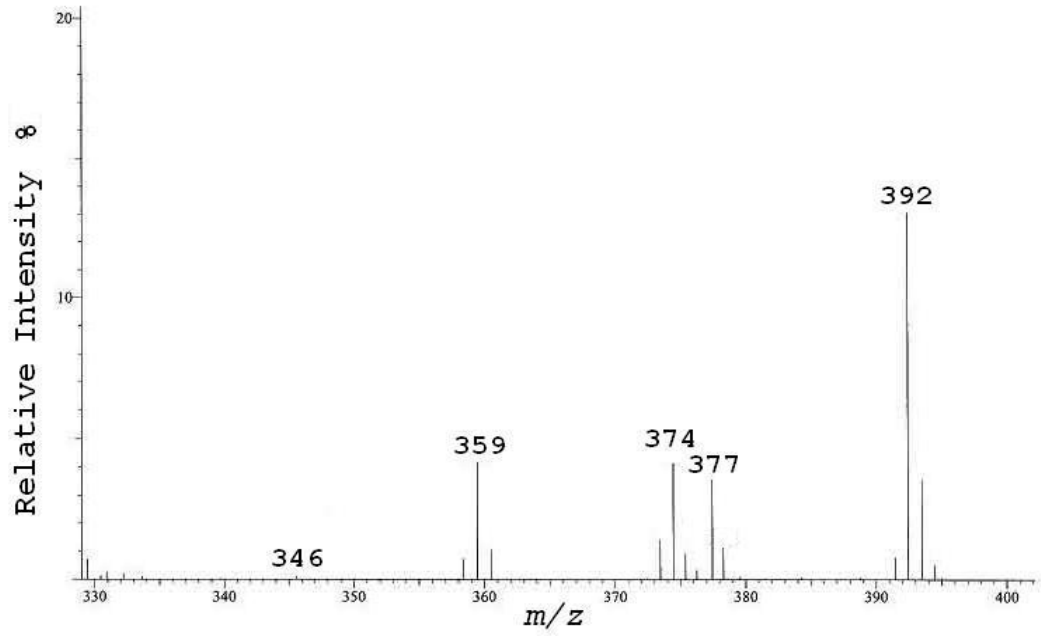

***Figure 4-7*: The DI/EI mass spectrum of deuterated cholesterol.**

As previously discussed, cholesterol was scanned over the mass range m/z 350-405. Over this range, the spectrum shows four prominent ions, M^+ (386 Da), $[M-15]^+$ (371 Da), $[M-18]^+$ (368 Da) and $[M-33]^+$ (353 Da) due to the loss of methyl group, water and water+methyl group respectively (**Figure 4-6**). As the deuterated cholesterol shows the same loss ion peaks with cholesterol (**Figure 4-8**), each peak group could potentially be used in quantification.

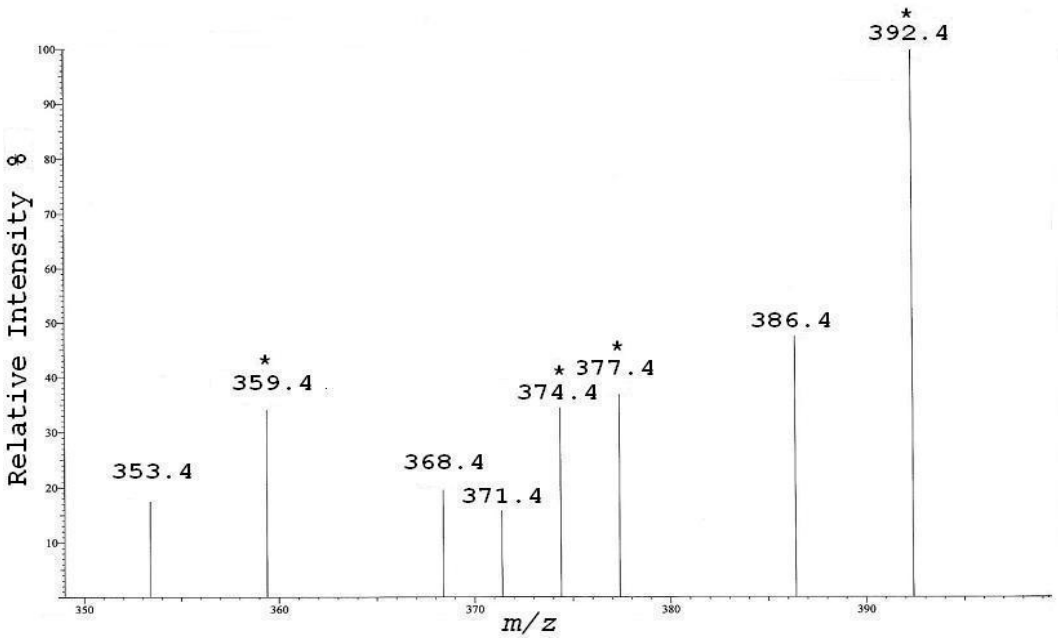

***Figure 4-8*: DI/EI mass spectrum of a mixture of standard cholesterol and deuterated cholesterol. Ions at m/z 386.4, 371.4, 368.4 and 353.4 represent the M^+, $[M-15]^+$, $[M-18]^+$ and $[M-33]^+$ for standard cholesterol respectively. Ion at m/z 392.4, 377.4, 374.4 and 359.4 represent the M^+, $[M-15]^+$, $[M-18]^+$ and $[M-33]^+$ for deuterated cholesterol respectively. (□Deuterated cholesterol-related peaks)**

4.2.5. Cholesterol Quantification

4.2.5.1. Standard Curve

A standard curve was prepared initially by using unlabelled cholesterol and deuterated cholesterol in mass ratios ranging from 0.1 to 3.0 (D0-cholesterol/D6-cholesterol). The mass range scanned was m/z 350-405 with 220 scans averaged for each sample. **Figure 4-9** shows the standard curves based on four different ion mass ratios, 386.4/392.4, 371.4/377.4, 368.4/374.4 and 353.4/359.4.

4.2.5.2. Cholesterol Quantification

For cholesterol quantification in lipid extracts, a known amount of the internal standard (deuterated cholesterol) was added to the lipid extract, and the peak area ratio was used to determine the amount of cholesterol present in the lipid extract by reference to a standard curve.

To gauge recovery, a known amount of the internal standard deuterated cholesterol was added into the sample tissue homogenate initially. Quantification results with the internal standard added initially, were compared with the results when the internal standard was added to the final $CHCl_3$/MeOH lipid extract.

4.3. Results and Discussion

4.3.1. Standard Curve Used for Determination of Cholesterol Quantification

Cholesterol was scanned over the mass range m/z 350-405. Four prominent ions were detected, M^+ (386 Da), the cholesterol ion and loss ions $[M-15]^+$ (371 Da), $[M-18]^+$ (368 Da) and $[M-33]^+$ (353 Da) due to the loss of methyl group, water and water+methyl group respectively. Deuterated cholesterol in the same range shows four corresponding peaks (**Figure 4-8**). Therefore, selected ion monitoring (SIM) runs

using DI/EI mass spectrometry were performed on these four different groups of ions: 386.4/392.4, 371.4/377.4, 368.4/374.4 and 353.4/359.4.

The standard curves for relative intensity ratio (D0/D6) versus mass ratio (D0/D6) were made for each ion group (**Figure 4-9**), and then plotted onto one graph (**Figure 4-10**) to allow the comparison of each slope. The regression (R^2) values showed all the data points had a good fit for the linear regression. However, the standard curve of the ion group 368.4/374.4 could not be used due to some interfering ions, which increase the ion peak of 368.4. These ions may originate from the other compounds in the extract (e.g. fatty acids). The standard curve of the ion group 386.4/392.4 was selected as the primary standard curve for quantification, due to the increased contrast of peak abundance compared with the background. The standard curve of the second largest peak group 371.4/377.4 was used to confirm the results. The standard curve of ion group 353.4/359.4 was not used in this study due to the low abundance compared with the background. In summary, the standard curves of ion groups 386.4/392.4 and 371.4/377.4 were used in all cholesterol quantification.

4.3.2. Cholesterol in Mammalian Lenses

In order to establish the cholesterol content of mammalian lenses, several animals were chosen. Samples of porcine, bovine, gallinaceous, ovine and human lens extracts were generously provided by Jane Deeley. **Figure 4-11** shows significant variation in

cholesterol concentration in the lenses between animal species. The cholesterol content in the bovine lens, ovine lens and porcine lens were similar, and each had a 2-fold greater content than that in the chicken lens.

The cholesterol concentration was much higher in the human lens, especially in old lens. The cholesterol concentration in the lens of a young human adult was approx 3-fold higher than that of the bovine, ovine and porcine lenses, and 5-fold higher than that of the chicken lens. These differences were more pronounced when compared to the cholesterol concentration of an elderly human lens, which was approximately 10 times higher than the bovine, ovine or porcine lenses, and ~17 times greater than gallinaceous lens.

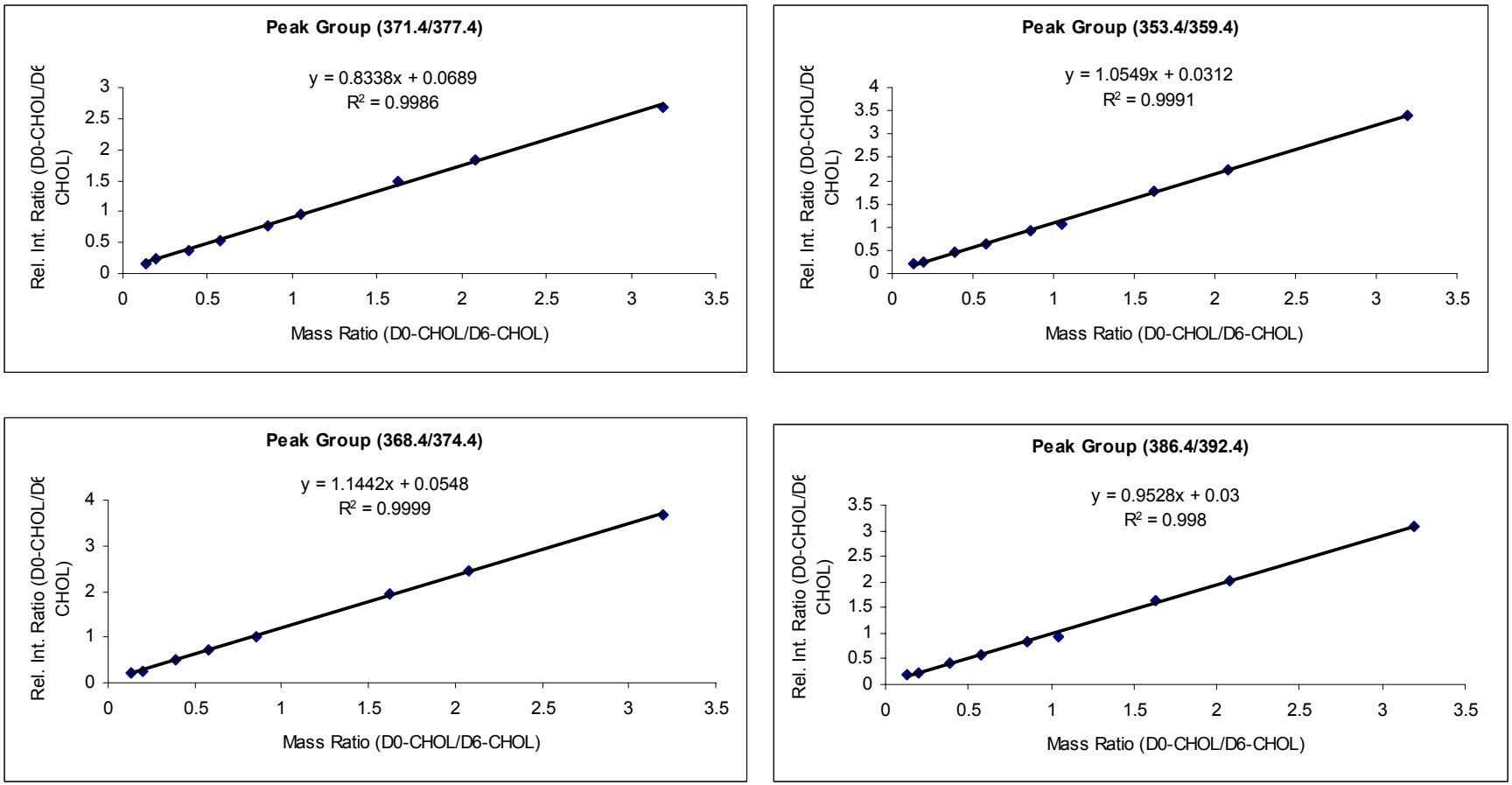

***Figure 4-9*: Plot of mass ratio vs. relative intensity ratio (D0-CHOL/D6-CHOL) for peak groups 371.4/377.4, 353.4/359.3, 368.4/374.4 and 385.4/392.4. (Linear regression equation: Rel. Int. Ratio (Y) = Slope×Mass Ratio (X) + Constant)**

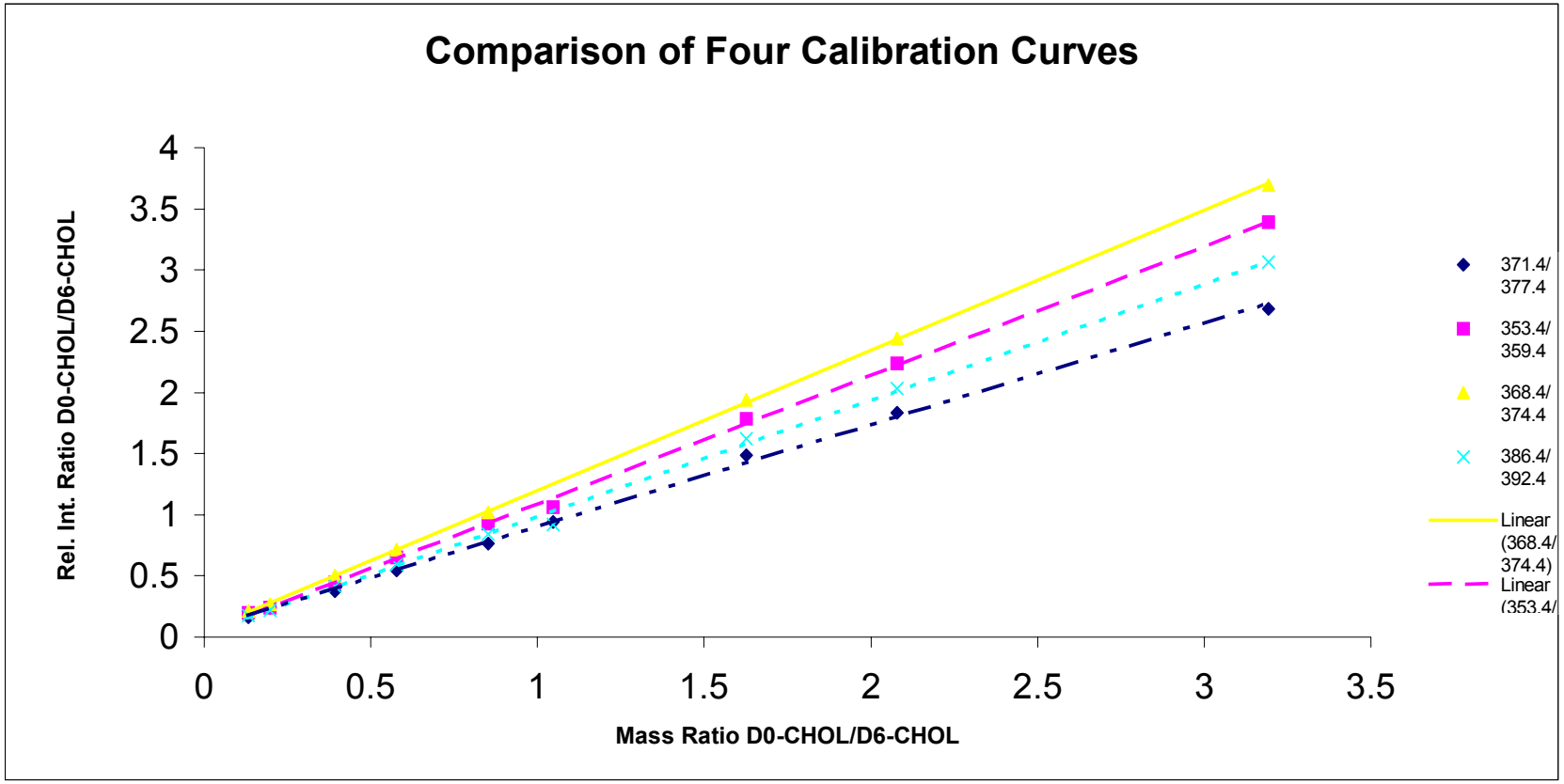

***Figure 4-10*: Integrated graph comparison of standard curve by plotting mass ratio from 0.1 to 3.0 vs. relative intensity ratio (D0-CHOL/D6-CHOL) for peak group 353.4/359.4, 371.4/377.4, 368.4/374.4 and 386.4/392.4.**

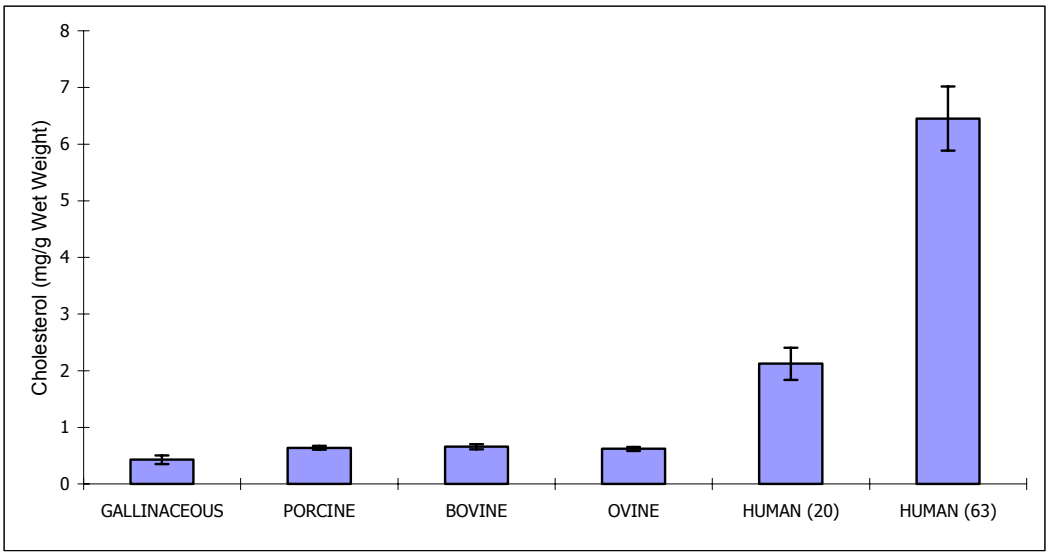

***Figure 4-11*: Cholesterol content of a variety of animal lenses. The human lenses used in this analysis were aged 20 and 63. The error bars represent one standard deviation of the mean (porcine n=3, bovine n=3, ovine n=3, gallinaceous n=4, human n=2)**

4.3.3. Determination of Cholesterol Losses during Extraction

To investigate the possible loss of cholesterol during the lipid extraction procedure, the concentrations of cholesterol from the same species were compared by adding the internal standard at different stages. The internal standard (deuterated cholesterol) was either added immediately after homogenization or added to the final $CHCl_3$/MeOH lipid extracts. The original tissues (~25 mg) were both obtained from the same region of one lamb lens.

Significant differences were observed in the cholesterol content between the additions

of the internal standard at the different stages (**Figure 4-12)**. Upon the addition of the internal standard after homogenization, an apparently 13-fold increase in cholesterol content was observed in comparison when the internal standard was added to the final extracts.

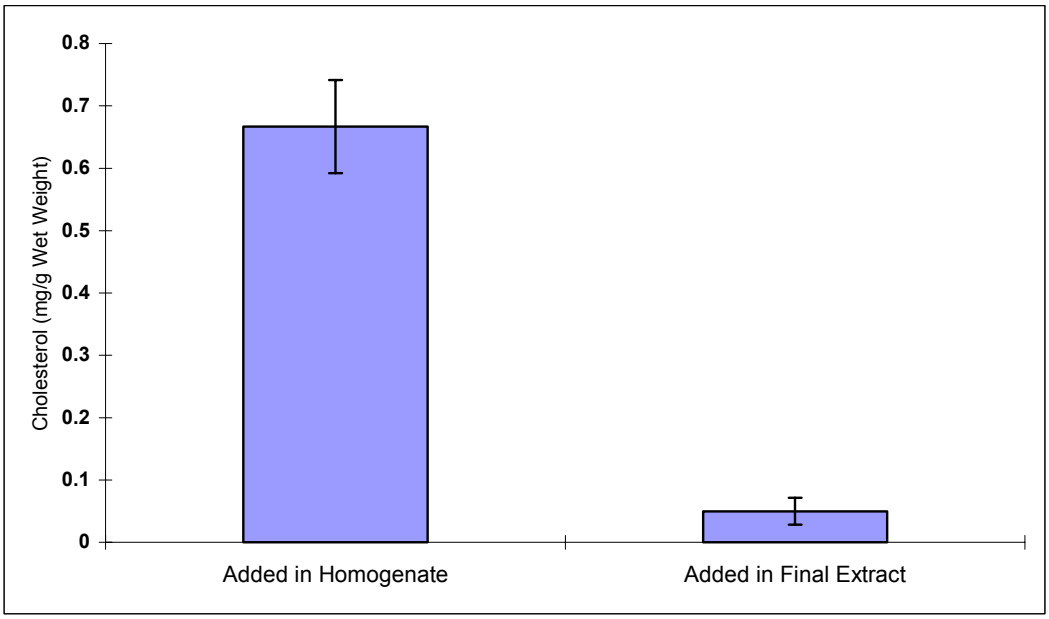

***Figure 4-12*: Cholesterol content of lamb lens with the addition of the internal standard after homogenization and to the final lipid extracts. The error bars represent one standard deviation of the mean (n=3).**

As both samples were extracted from the same region of a single lens, cholesterol content should be similar. However, the results revealed an enormous difference, suggesting there was a significant loss of cholesterol during the lipid extraction procedure. The cholesterol lost may be due to the cholesterol being not fully extracted from the original tissue and/or the cholesterol adsorbing onto the internal surface of the glass extraction tube. It is unlikely that the cholesterol is in the aqueous phase,

however this was not examined. The cholesterol may also react with other compounds in the homogenate, which may lead to a lowering of cholesterol content. However, the loss of internal standard (deuterated cholesterol) during lipid extraction may contribute to errors. In order to determine whether the loss of deuterated cholesterol affected the quantitative result, the recovery of deuterated cholesterol was investigated (see section **4.3.4.**).

Figure 4-13 shows the cholesterol content obtained from the same lamb lens sample. Both lens samples (~25 mg) were extracted using either a 10 mL and 2 mL extraction tube. The cholesterol content using the 10 mL extraction tube was significantly lower than a 2 mL extraction tube. This result confirms one hypothesis of loss of cholesterol during lipid extraction, that cholesterol tends to stick onto the internal surface of the glass extraction tube. Reduction of the internal surface area by using a smaller volume extraction tube was shown to increase the cholesterol recovery. Thus, all the lens samples (with the exception of the animal lens lipid extracts from Jane Deeley used in **4.3.2.**) used in this study (approximately 25 mg by weight) were extracted using 2 mL extraction tubes.

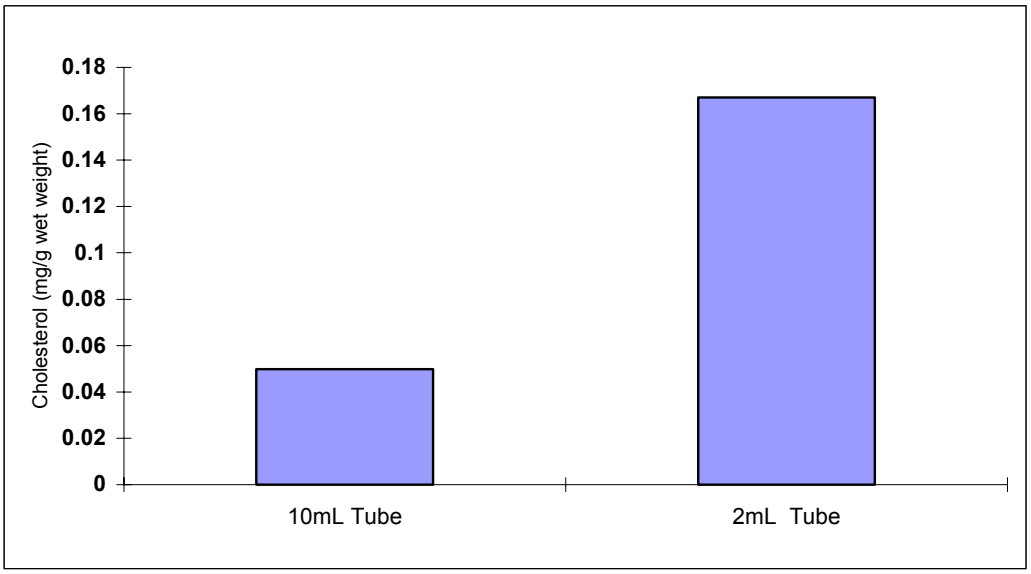

***Figure 4-13*: Cholesterol content of a lamb lens sample extracted using a 10 mL and a 2 mL tube.**

4.3.4. Recovery of Internal Standard (Deuterated Cholesterol)

To determine the loss of internal standard loss during the lipid extraction procedure, the recovery of deuterated cholesterol was tested. 7-ketocholesterol (3β-hydroxy-5-cholesten-7-one) was used as an additional internal standard due to its similarity to deuterated cholesterol. The stock solution of 7-ketocholesterol and deuterated cholesterol mixture (~1:1 mass ratio) was scanned over the mass range m/z 340-450. The ion peaks M^+ (400 Da) from 7-ketocholesterol and M^+ (392 Da) from deuterated cholesterol were used in this recovery study. The relative response (mass ratio/peak area ratio), therefore, can be determined and used to determine deuterated cholesterol recovery (details see Appendix D).

Lamb lens tissue samples (~25 mg, quadruplicate) were used in the deuterated cholesterol recovery test. Known amounts of deuterated cholesterol were added to the samples immediately after homogenization. By contrast, the 7-ketocholesterol was added to the final extract. The actual amount of deuterated cholesterol was then calculated (details see Appendix D). The recovery efficiency of deuterated cholesterol in the sample weight range 15-30 mg was found to be 57.7 +/- 4.78%.

This study proves that there is loss of internal standard during the lipid extraction procedure. There is approximately 58% recovery of cholesterol using this method.

4.3.5. Cholesterol in the Human Lens

In this study, the cholesterol contents of three different regions (nucleus, barrier and cortex) in the human lens were analysed (details of sectioning the human lens see Appendix F). A young, a middle aged and an old lens was examined. The result of this study revealed that differences in the cholesterol content exist between different regions of the human lens. These differences were much less pronounced in the young lens. The nuclear region appears to have the highest cholesterol content, and the cortex has the lowest (**Figure 4-14**). This is in broad agreement with previously published data, which reveals higher cholesterol content in the nuclear region.[55]

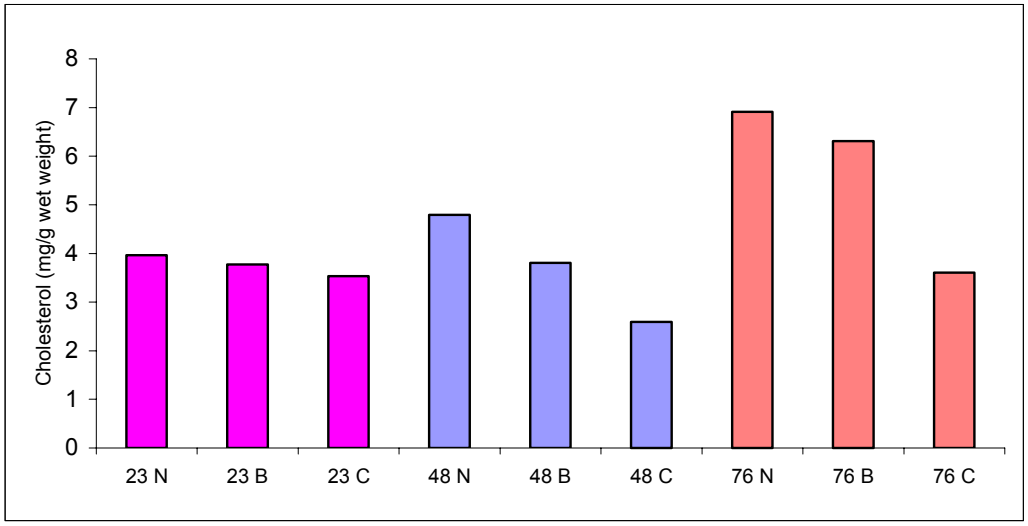

***Figure 4-14*: Cholesterol content in nucleus, barrier and cortex region of human lenses of age 23, 48 and 76 years. (n=1) (N=nucleus, B=barrier and C=cortex)**

It was also observed that the old human lens contained more cholesterol than the young human lens in nuclear and barrier region (approximately 2-fold higher). However, there appeared to be little cholesterol content change in cortex region with age.

As previously mentioned, cholesterol functions to modulate the physical properties of the cell plasma membrane, such as rigidity and fluidity. With age, the increase of the cholesterol content may lead to a decrease in the transport of ions and organic solutes, as a result of a decrease in membrane fluidity.[66, 67] Higher cholesterol content in the lens membrane has been considered to promote the structural rigidity of the cell membrane by disordered membrane lipids.[68]

The increase in the cholesterol content in the human lens with age, especially in the nucleus, may explain some of the physical changes that occur with age in the lens.

These age-related changes may underlie pathologies of the aged human lens, such as presbyopia and cataract.

Due to time limitation only a small test group of human lenses were used in this study. More lenses, would need to be analysed to confirm the trend found in the above results.

4.4. Conclusions

A technique for the rapid quantification of cholesterol content in lipid extracts using DI/EI mass spectrometry was developed in this study. Results obtained using this method are in broad agreement with previously published data using more traditional methods.[69, 70, 71, 72] Investigations showed there is a ~58% recovery of cholesterol during the extraction procedure.

This study profiled the cholesterol content of bovine, ovine, porcine, gallinaceous and human lenses with differences observed between species. The concentration of cholesterol in the human lens was observed to be significantly greater than that in other mammalian lenses. This observation may demonstrate that other mammalian lenses are not likely to be good models for the investigation of age-related pathologies of the human lenses such as cataract and presbyopia. These mammalian lenses are however, valuable for the establishment of methods to be used for the human lens analysis.

The cholesterol content in nucleus, barrier and cortex regions of the human lens was investigated, as well as the changes with age. The nucleus contained the highest cholesterol content in the human lens, and the cortex had the lowest cholesterol content. A significant increase of the cholesterol content was observed in the nucleus and barrier region of the human lens with age. The difference between the internal regions (nucleus and barrier) and the cortex appear to increase markedly with age.

In summary, this study has demonstrated numerous differences in cholesterol content in different regions of the human lens and a significant increase with age. This suggests that the fibre cell plasma membrane may play an important role in age-related changes of the human lens. In addition, it suggests that other mammalian lenses may be poor candidates as models for the study of lipid membrane disorders in the human lens due to the significant differences in cholesterol content.

Appendix A

Calculation of flux value (**J**) with raw data

Number of samples	Time of exposure (**t**) min	Quantity of substance crossing membranes (**D**) dpm		Flux values (**J**) dpm•cm^{-2}•min^{-1}	
		24 y.o.	74 y.o.	24 y.o.	74 y.o.
1	0	50	72	0	0
2	150	113	154	2.1	2.7333
3	330	262	366	3.212121	4.454545
4	510	534	547	4.745098	4.656863
5	810	1023	1026	6.006173	5.888889
6	1080	1480	1590	6.62037	7.027778
7	1260	2087	2686	8.083333	10.37302
8	1980	3380	4443	8.409091	11.03788
9	2700	5972	5934	10.96667	10.8556
10	3420	8096	7355	11.76316	10.64766

Note: exposed membrane areas for all the samples are same (**A** = 0.2 cm^2).

Appendix B

This standard curve was used for the determination of PSH content in the lens samples.

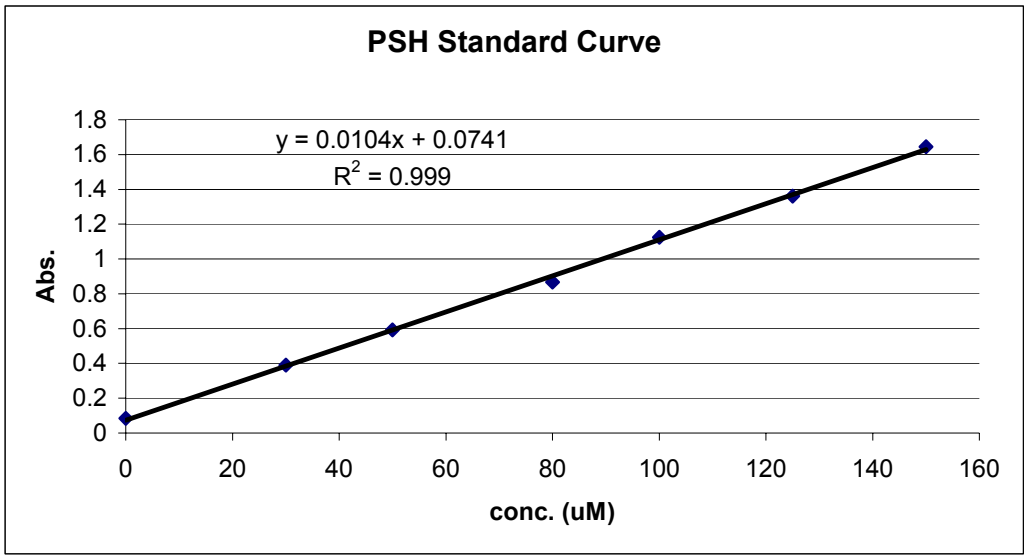

Figure A: **Standard curve for Protein Sulphydryl assay.**

This standard curve was used for the determination of total protein content in the lens samples.

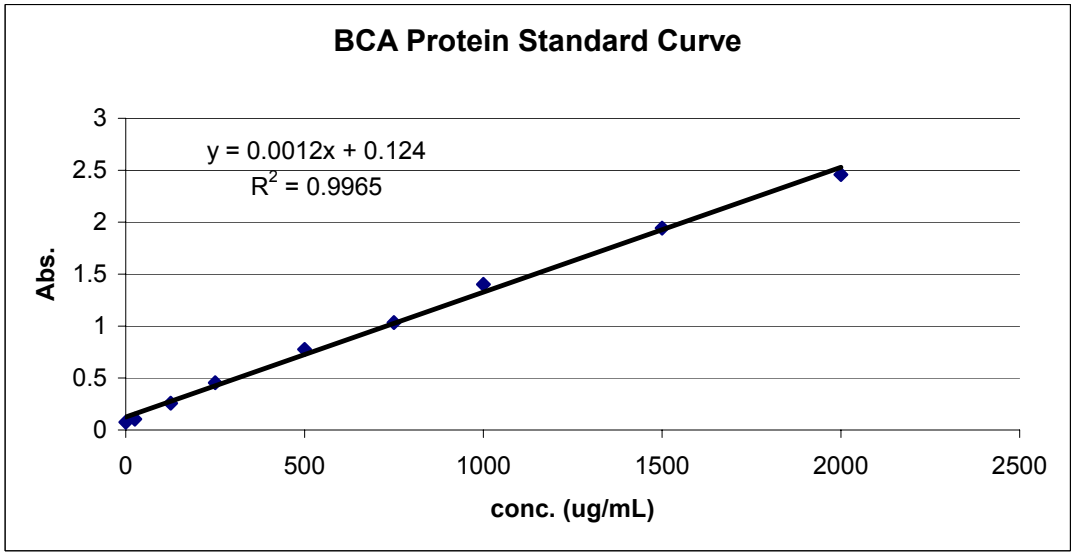

Figure B: **Standard curve for BCA protein assay.**

Appendix C

Protocol of Coomassie Protein Assay

BSA standards were used in the Coomassie Protein Assay and in the BCA Protein Assay (detail see section **3.2.1.**). Standards or protein samples (5 μL) were pipetted into the appropriate microplate wells. 250 μL aliquots Coomassie Reagent was added to each well, and the plate was mixed thoroughly for ~30 seconds. The plate was incubated at room temperature for 10 minutes. The absorbances of the solutions were measured at 595 nm on the plate reader. A standard curve was prepared by plotting the Absorbance against BSA concentrations (μg/mL), and the standard curve was used to calculate the protein concentration of each sample.

Appendix D

Calculations of Deuterated Cholesterol Recovery Efficiency

1) Stock solution (mixture of D6-Chol. and Keto-Chol.)

Known amount of D6-Chol. and Keto-Chol.was added:

Mass of Keto-Chol. = 38.1 μg; Mass of D6-Chol. = 40.2 μg

 Actual mass ratio = mass of Keto-Chol./mass of D6-Chol. = 0.947

Then,

Run mass spectrometry using stock solution. Peak area ratio measured to be = 0.77

Then,

Convert Peak area ratio to Mass ratio by:

Mass ratio = Peak area ratio × Relative response

 Relative response = Mass ratio/Peak area ratio = 1.23

2) Sample (example)

Known amount of D6-Chol. and Keto-Chol.was added:

Mass of Keto-Chol. = 34.6 μg; Mass of D6-Chol. = 40 μg

Then,

Run mass spectrometry using extract. Peak area ratio measured to be = 1.09

Then,

Convert Peak area ratio to Mass ratio by,

Mass ratio (in final extract) = Mass of Keto-Chol./Mass of D6-Chol. = Peak area ratio × Relative response = 1.34

 Mass of Keto-Chol. (in final extract) = Mass of Keto-Chol. (added)

 Mass of D6-Chol. (in final extract) = Mass of Keto-Chol./Relative response = 25.81 μg

 Recovery efficiency = Mass of D6-Chol. (in final extract)/Mass of D6-Chol. (added) = 64.5%

Appendix E

Direct insertion (DI) methods in mass spectrometry

In direct insertion methods, the sample (e.g. 1 μL of solution) is deposited onto the tip of a glass capillary. The solvent is allowed to evaporate and the dried sample was then inserted directly into the heated ion source of the mass spectrometer via an air lock. The application of heat to the sample in the vacuum environment of the ion source results in volatilisation or thermal decomposition. The volatile molecules can then be ionised directly by either EI or CI methods.

Direct insertion is the simplest method of sample introduction, with the positioning of the sample in the source and the rate of temperature increase the most important variables to ensure obtaining reproducible results. This method is not appropriate for non-volatile compounds such as phospholipids as they decompose rather than vaporise at elevated temperatures (~350°C).

Appendix F

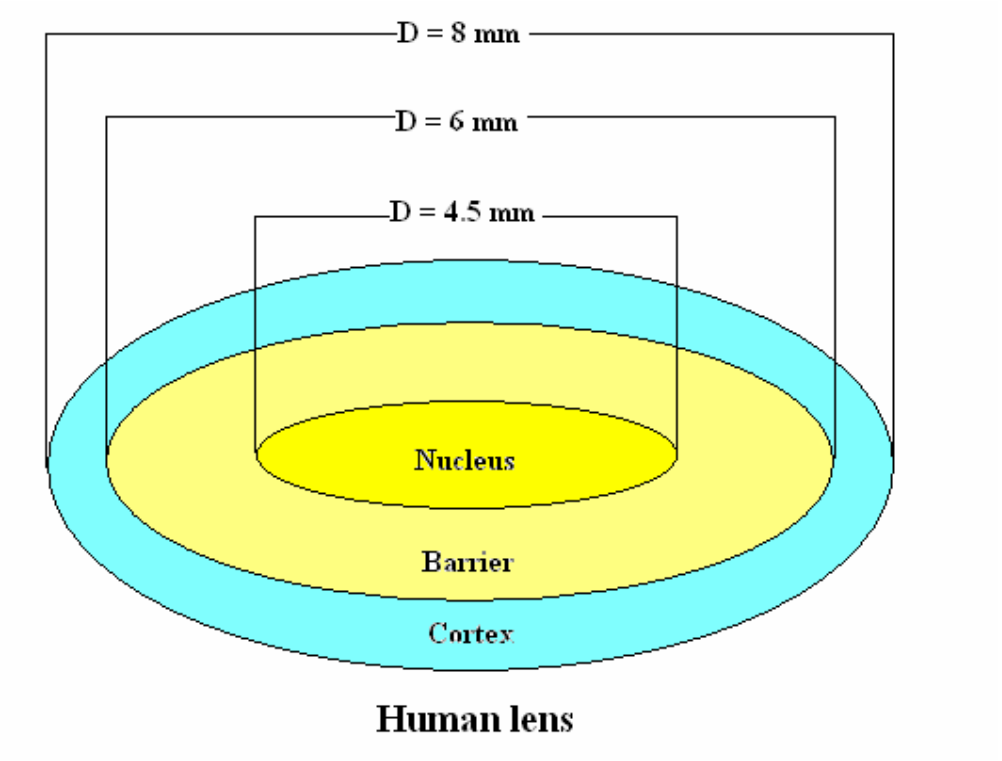

The diagram shows the human lens sectioning into nucleus, barrier and cortex.

LIST OF REFERENCES

(1) Tripathi, R. C., and Tripathi, B. J., Anatomy of the human eye, orbit and adnexa, pp 55-63, Academic Press Inc., London, U.K., **1984**

(2) Gaillard, E. R., Zheng, L., Merriam, J. C., and Dillon, J., Age-related changes in the absorption characteristics of the primate lens, *Investigative Ophthalmology and Visual Science,* **2000**, 41:1454-1459

(3) van Heyningen, R., The human lens, 3. Some observations on the post-mortem lens, *Experimental Eye Research*, **1972**, 13:155-160

(4) Taylor, A., Nutritional and environment influences on the eye, Chapter 1, CRC PRESS, N.Y., **1999**

(5) Heys, K. R., Cram, S. L., and Truscott, R. J. W., Massive increase in the stiffness of the human lens nucleus with age: the basis for presbyopia?, *Molecular Vision*, **2004**, 10:956-963

(6) Miesbauer, L., Zhou, X. J., Yang, Z.C., Yang, Z.Y., Sun, Y. P., Smith, D., and Smith, J., Posttranslational modifications of water soluble human lens crystallins from young adults, *Journal of Biological Chemistry*, **1994**, 269:12494-12502

(7) Latina, M., Chylack, L., Fagerholm, P., Nishio, I., Tanaka, T., and Palmquist, B., Dynamic light scattering in the intact rabbit lens. Its relation to protein concentration, *Investigative Ophthalmology and Visual Science*, **1987**, 28:175-183

(8) Delaye, M., and Tardieu, A., Short-range order of crystallin proteins accounts for eye lens transparency, *Nature*, **1983**, 302:415-417

(9) Bloemendal, H., de Jong, W., Jaenicke, R., Lubsen, N. H., Slingsby, C., and Tardieu, A., Aging and vision: structure, stability and function of lens crystallins, *Progress in Biophysics and Molecular Biology*, **2004**, 86:407-485

(10) Groenen, P. J., Merck, K., de Jong, W., and Bloemendal, H., Structure and modifications of the junior chaperone α-crystallin. From lens transparency to molecular pathology, *European Journal of Biochemistry*, **1994**, 225:1-19

(11) Harding, J., and Crabbe, M. J., The lens: development, proteins, metabolism and cataract. *The Eye*, pp207-492, Academic Press Inc., London, U.K., **1984**

(12) Wistow, G. J., and Piatigorsky, J., Lens crystallins: the evolution and expression of proteins for a highly specialized tissue, *Annual Review of Biochemistry*, **1988**, 57:479-504

(13) Truscott, R. J. W., and Augusteyn, R. C., Changes in human lens proteins during nuclear cataract formation, *Experimental Eye Research*, **1977**, 24:159-170

(14) Collier, R., and Zigman, S., in Degenerative retinal disorders: clinical and laboratory investigations, Alan Liss, N.Y., **1987**

(15) Garner, B., Vazquez, S., Griffith, R., Lindner, R. A., Carver, J. A., and Truscott, R. J. W., Identification of Glutathionyl-3-hydroxykynurenine glucoside as a novel fluorophore associated with aging of the human lens, *Journal of Biological Chemistry*, **1999**, 274:2084-20854

(16) Sweeney, M. H., and Truscott, R. J., An impediment to glutathione diffusion in older normal human lenses: a possible precondition for nuclear cataract, *Experimental Eye Research*, **1998**, 67:587-595

(17) Johnson, G. J., Limitations of epidemiology in understanding pathogenesis of cataracts, *Lancet*, **1998**, 351:925-926

(18) Donnelly, C. A., Seth, J., Clayton, R. M., Phillips, C. I., Cuthbert, J., and Prescott, R. J., Some blood plasma constituents correlate with human cataract, *British Journal of Ophthalmology*, **1995**, 79:1036-1041

(19) WHO, Management of cataract in primary health care services, *World Health Organization*, **1990**

(20) Oliff, H., Cataract, *Ophthalmic Genetics Newsletter*, 1(2), National Institute of Health (U.S.), **2000**

(21) Moffat, B. A., Landman, K. A., Truscott, R. J., Sweeney, M. H., and Pope, J. M., Age-related changes in the kinetics of water transport in normal human lenses, *Experimental Eye Research*, **1999**, 69:663-669

(22) Truscott, R. J. W., Age-related nuclear cataract-oxidation is the key, *Experimental Eye Research*, **2005**, 1-17

(23) Cussler, E. L., Diffusion: mass transfer in fluid system, Models for diffusion, 3rd Ed., Cambridge University Press, Cambridge, U.K., **1997**

(24) Truscott, R. J., Age-related nuclear cataract: a lens transport problem, *Ophthalmic Research*, **2000**, 32:185-194

(25) Verkman, A. S., Water permeability measurement in living cells and complex tissues, *The Journal of Membrane Biology*, **2000**, 173:73-87

(26) Agre, P., and Kozono, D., Aquaporin water channels: molecular mechanisms for human diseases, *Federation of European Biochemical Societies*, **2003**, 555:72-78

(27) Van der Bijl, P., Thompson, I. O., and Squier, C. A., Comparative permeability of human vaginal and buccal mucosa to water, *Europe Journal of Oral Science*, **1997**, 105:571-575

(28) Addicks, W. J., Flynn, G. L., and Weiner, N., Validation of a flow-through diffusion cell for use in transdermal research, *Pharmaceutical Research*, **1987**, 4:337-341

(29) Kobayashi, Y., and Maudsley, D. V., Biological applications of liquid scintillation counting, Chapter 2, Academic Press, N.Y., **1974**

(30) Garner, M. H., and Spector, A., Selective oxidation of cysteine and methionine in normal and senile cataractous lenses, *Proceedings of the National Academy of Science, U.S.A.*, **1980**, 77:1274-1277

(31) Truscott, R. J. W., and Augusteyn, R. C., The state of sulphydryl groups in normal and cataractous human lenses, *Experimental Eye Research*, **1977**, 25:139-148

(32) Truscott, R. J. W., and Augusteyn, R. C., Oxidative changes in human lens proteins during senile nuclear cataract formation, *Biochemica et Biophysica. Acta*, **1977**, 492:43-52

(33) Thomson, J. A., and Augusteyn, R. C., Ontogeny of human lens crystallins, *Experimental Eye Research*, **1985**, 40(3):393-410

(34) Harrington, V., McCall, S., Huynh, S., Srivastava, K., and Srivastava, O. P., Crystallins in water soluble-high molecular weight protein fractions and water

insoluble protein fractions in aging and cataractous human lenses, *Molecular Vision*, **2004**, 10:476-489

(35) Giblin, F. J., Padgaonkar, V. A., Leverenz, V. R., Lin, L. R., Lou, M. F., Unakar, N. J., Dank, L., Dickerson, J. E. Jr., and Reddy, V. N., Nuclear light scattering, disulfide formation and membrane damage in lenses of older guinea pigs treated with hyperbaric oxygen, *Experimental Eye Research*, **1995**, 60:219-235

(36) Spector, A., and Garner, W. H., Hydrogen peroxide and human cataract, *Experimental Eye Research*, **1981**, 33:637-681

(37) Berman, E. R., Biochemistry of the eye, pp 24-25, Plenum Press, N.Y., **1991**

(38) Eaton, J. W., Is the lens canned?, *Free Radical Biology & Medicine*, **1991**, 11:207-213

(39) McNulty, R., Wang, H., Mathias, R., Ortwerth, B. J., Truscott, R. J. W., and Bassnett, S., Regulation of tissue oxygen levels in the mammalian lens, *The Journal of Physiology*, **2004**, 559:883-898

(40) Lane, N., Oxygen: the molecule that made the world, Oxford University Press, N. Y., **2002**

(41) Immo, S. E., Mitochondria, A John Wiley & Sons, Inc., N.Y., **1999**

(42) Carroll, M., Organelles, Guildford Press, N. Y., **1989**

(43) Shoubridge, E. A., Nuclear genetic defects of oxidative phosphorylation, *Human Molecular Genetics*, **2001**, 10:2277-2284

(44) Barron, M., and Turnbull, D., Mitochondria and aging, aging at the molecular level, pp91-106, Kluwer Academic Publishers, Dordretch, The Netherlands, **2003**

(45) Brand, M. D., Chien, L. F., Ainscow, E. K., Rolfe, D. E., and Porter, R. K., The causes and functions of mitochondrial proton leak, *Biochemica et Biophysica. Acta*, **1994**, 1187

(46) Brand, M. D., Brindle, K. M., Buckingham, J. A., Harper, J. A., and Rolfe, D. F., The significance and mechanism of mitochondrial proton conductance, *International Journal of Obesity*, **1999**, 23:S4-S11

(47) Truscott, R. J., and Augusteyn, R. C., The state of sulphydryl groups in normal and cataractous human lenses, *Experimental Eye Research*, **1977**, 24(2):159-170

(48) Chen, Y. C., Reid, G. E., Simpson, R. J., and Truscott, R. J., molecular evidence for the involvement of alpha crystalline in the colouration/crosslinking of crystallins in age-related nuclear cataract, *Experimental Eye Research*, **1997**, 65(6):835-40

(49) Swartz, H. M., and Dunn, J. F., Measurements of oxygen in tissues: overview and perspectives on methods, *Advances in Experimental Medicinal Biology*, **2003**, 530:1-12

(50) Sedlak, J., and Linsay, R. H., Estimation of total protein bound and non-protein sulfhydryl groups in tissues with ellmans reagent, *Analytical Biochemistry*, **1968**, 25:192-205

(51) Berry, Y., and Truscott, R. J. W., The presence of a human UV filter within the lens represents an oxidative stress, *Experimental Eye Research*, **2001**, 72(4):411-421

(52) Mattews, C. K., van Holde, K. E., and Ahern, K. G., Biochemistry, 3rd ed.,

Benjamin Cummings, San Francisco, **2000**

(53) Yeagle, P. L., In the structure of biological membranes, Yeagle, P. L. ed., CRC Press, U.S.A., **2005**

(54) Zigman, S., Paxhia, T., Marinetta, G., and Girsch, S., Lipids of human lens fibre cell membranes, *Current Eye Research*, **1984**, 3:887-896

(55) Tang, D., Borchman, D., Yappert, M. C., and Cenedella, R. J., Influence of cholesterol on the interaction of alpha-crystallin with phospholipids, *Experimental Eye Research*, **1998**, 66:559-567

(56) Fisher, R. F., The significance of the shape of the lens and capsular energy changes in accommodation, *The Journal of Physiology*, **1969**, 201:21-47

(57) Coleman, D. J., Unified model for accommodative mechanism, *American Journal of Ophthalmology*, **1970**, 69:1063-1079

(58) Bova, L. M., Sweeney, M. H., Jamie, J. F., and Truscott, R. J., Major changes in human ocular UV protection with age, *Investigative Ophthalmology and Visual Science*, **2001**, 42:200-205

(59) Borchman, D., Byrdwell, C., and Yappert, C., Regional and age-dependent differences in the phospholipids composition of human lens membranes, *Investigative Ophthalmology and Visual Science*, **1994**, 35:3938-3942

(60) Zelenka, P. S., Lens lipids, *Current Eye Research*, **1984**, 3:1537-1559

(61) Borchman, D., Yappert, M. C., and Afzal, M., Lens lipids and maximum lifespan, *Experimental Eye Research*, **2004**, 79:761-768

(62) de Hoffman, E., and Stroobant, V., Mass spectrometry principles and applications, Wiley, U.K., **2002**

(63) Herbert, C. G., and Johnstone, R. A. W., Mass spectrometry basics, CRC Press, U.S.A., **2003**

(64) Harris, D. C., Quantitative chemical analysis, 6th ed., W. H. Freeman and Co., California, U.S.A., **2003**

(65) Folch, J., Lees, M., and Sloane Stanley, G. H., A simple method for the isolation and purification of total lipids from animal tissues, *Journal of Biological Chemistry*, **1957**, 226:497-509

(66) Yeagle, P. L., Cholesterol and the cell membrane, *Biochemica et Biophysica. Acta*, **1985**, 822:267-287

(67) Yuli, T., Wilbrandt, W., and Shinitzly, M., Glucose transport through cell membranes of modified lipid fluidity, *Biochemistry*, **1981**, 20:4250-4256

(68) Lippert, J. L., and Peticolas, W. L., Laser raman investigation of the effect of cholesterol on conformational changes in dipalmitoyl lecithin multilayers, *Proceedings of the National Academy of Science of U.S.A.*, **1971**, 68:1572-1576

(69) Li, L. K., So, L., and Spector, A., Membrane cholesterol and phospholipid in individual bovine lenses, *Current Eye Research*, **1987**, 6:599-605

(70) Andrews, J. S., and Leonard-Martin, T., Total lipid and membrane lipid analysis of normal animal and human lenses, *Investigative Ophthalmology and Visual Science*, **1981**, 21:39-45

(71) Cotlier, E., Obara, Y., and Toftness, B., Cholesterol and phospholipids in protein fractions of human lens and senile cataracts, *Biochemica et Biophysica. Acta*, **1978**, 530:267-278

(72) Duncan, G., Mechanisms of cataract formation in the human lens, Chapter 6, Academic Press Inc., London, U.K., **1981**

(73) http://www.opricsreport.com/content/article.php?article_id=1006, computer image, accessed 06/06/04

(74) http://www.uow.edu.au/science/chem/acrf, computer image, accessed 18/08/05

(75) McMurry, J., and Castellion, M., Fundamentals of general, organic and biological chemistry, 3rd ed., Prentice Hall, New Jersey, U.S.A., **2002**

(76) Brown, N. P., and Bron, A. J., Lens disorders, a clinical manual of cataract diagnosis, Nutterworth-Heinemann, Oxford, **1996**

(77) http://www.vision-surgery.com/conditions-presbyopia.html, computer image, accessed 28/01/06